Boundary layer contribution to the Magnus effect on a spinning cylinder at low angles of attack

by

Howard Leon Power, Jr.

A Dissertation Submitted to the

Graduate Faculty in Partial Fulfillment of

The Requirements for the Degree of

DOCTOR OF PHILOSOPHY

Major Subjects: Aerospace Engineering
Mechanical Engineering

Approved:

Signature was redacted for privacy.

In Charge of Major Work

Signature was redacted for privacy.

For the Major Departments

Signature was redacted for privacy.

For the Graduate College

Iowa State University
Ames, Iowa

1971

TABLE OF CONTENTS

NOMENCLATURE

C_{P_0}	surface pressure coefficient
C_Y	total sideforce coefficient based on frontal area
C_{Y_1}	displacement thickness effect on sideforce coefficient
C_{Y_2}	radial pressure gradient effect on sideforce coefficient
C_{Y_3}	skin friction effect on sideforce coefficient
C_{Y_4}	circulation effect on sideforce coefficient
d	diameter of the cylinder
f	velocity profile function
f	circulation function
F	integral of velocity profile function
g	velocity profile function
G	integral of velocity profile function
H	velocity profile function
$\mathcal{H}$	integral of the velocity profile function
k	inviscid circulation distribution function
K	velocity profile function
$\mathcal{K}$	integral of the velocity profile function
L	length of cylinder
L	velocity profile function

M	velocity profile function
$\mathcal{M}$	integral of the velocity profile function
N	velocity profile function
$\mathcal{N}$	integral of the velocity profile function
p	pressure
$\bar{p}$	dimensionless spin rate
P	velocity profile function
$\mathcal{P}$	integral of the velocity profile function
q	freestream dynamic pressure
Q	velocity profile function
$\mathcal{Q}$	integral of the velocity profile function
r	radial coordinate
r_0	radius of the cylinder
R_0	radius of the boundary layer edge
R_L	Reynolds number based on the cylinder length
R_C	crossflow Reynolds number based on the cylinder diameter
t	time
T	velocity profile function
$\mathcal{T}$	integral of the velocity profile function
u	axial component of velocity
U	freestream air velocity
v	radial component of velocity

V	surface velocity of the cylinder
w	azimutal component of velocity
x	axial component
Y	side force
z	velocity profile function
Z_1	integral of velocity profile function
α	angle of attack
β	velocity profile function
γ	velocity profile function
Δ	displacement thickness
δ	boundary layer thickness
ϵ	velocity profile function
η	transformed radial component
λ	velocity profile function
μ	coefficient of viscosity
ν	kinematic viscosity coefficient
ξ	transformed axial coordinate
ρ	air density
τ	surface shearing stress
φ	azimuthal coordinate
ω	spin angular velocity

INTRODUCTION

The study of flight trajectories of spinning shells and missiles requires a complete knowledge of the aerodynamic forces developed during their flight. It has long been recognized that when such a body is at an angle of attack spin introduces an aerodynamic side force and moment. This is what is now commonly known as the "Magnus effect". The prediction of these forces and moments for a general case is a very complicated problem. For this reason the only theory developed to date assumes low angles of attack and is based on the development of a laminar boundary layer that has not separated. This theory has not been particularly accurate in the prediction of the Magnus effects. Hence, this study was made in an attempt to improve the situation by providing better information concerning these effects.

HISTORICAL BACKGROUND

In 1730 B. Robins (19) expressed the opinion that the lateral deviation of the flight path of a cannon ball was due to its spin. This was probably the first explanation of what is now called "Magnus effects". In 1853 Magnus' (13) experimental investigations with spinning cylinders proved that the spin produced a force in a direction perpendicular to the normal velocity. Thus it appeared that the spin did cause the deviations. Lord Rayleigh (18) was the first to mathematically describe Magnus effects. He did this by combining a potential flow with circulation. He was careful to note, however, that his solution was not valid for a viscous fluid. In his theory no mechanism for the development of the needed circulation was available so that the relationship between the spin rate and the resulting lift was a mystery.

In 1918 Prandtl (17) studied the problem and demonstrated that the circulation could be developed by boundary layer vorticity being shed by separation. In this case the net vorticity of the shed boundary layer was equal to the resulting circulation but of opposite sign. Once the role of the boundary layer in creating the circulation was determined, Wood (23) studied boundary layers for which the streamlines were closed. He found that the circulation imparted to the inviscid flow was less than that of the circulation of the motion at the boundary. Glauert (4) solved the rotating cylinder problem and his results for the ratio of the cylinder velocity

to the circulation velocity were the same as predicted by Wood. More recently, a numerical analysis of an impulsively rotated cylinder immersed in a uniform free-stream was performed by Thoman and Szewczyk (22). They presented streamline patterns for various Reynolds numbers, cylinder speed to freestream speed ratios, and time. From these solutions the cylinder lift coefficient as a function of time may be estimated. It is this result that has a direct application to the crossflow of a spinning cylinder at low angles of attack.

Howarth (6) studied the boundary layer solution for a rotating sphere in still air as well as that for a rotating cylinder at zero angle of attack. Experimental investigations by Gowen and Perkins (5) and Dunn (3) have demonstrated that the normal force due to crossflow of a high fineness ratio body at low angles of attack developes with distance along the body much the same as the flow developes about an impulsively-translating circular cylinder. Kelly's (9) work for predicting the normal force on a non-spinning cylinder at an angle of attack used this approach. Platou (16) and Buford (1) have both suggested that the crossflow component of the boundary layer for spinning bodies can be approximately assumed to be independent of the axial component. For this reason the crossflow of a spinning cylinder at low angles of attack may be represented by an impulsively rotated cylinder.

Martin (14) used a perturbation solution for the estimation of the boundary layer displacement thickness contribution to the Magnus force and

moment on a spinning cylinder at low angles of attack. This work was extended by Kelly (10) and Kelly and Thacker (11). Both of these works neglected the inviscid axial circulation development predicted by the impulsively rotated cylinder solution. The work described in this thesis carries Kelly's solution to a higher order of approximation and includes the effects of the inviscid circulation development.

ANALYTICAL INVESTIGATION

Equations of Motion

In this investigation boundary-layer theory is used to study the exterior flow about an open-end rotating cylinder as shown in Figure 1a. A nonrotating cylindrical coordinate system with the x axis along the longitudinal or spin axis of the cylinder is used. The r coordinate is assumed to be perpendicular to the cylinder surface and the azimuth angle coordinate is labeled φ. The uniform free stream velocity U is inclined at a small angle of attack α and the cylinder is assumed to be spinning at a nondimensional roll rate $\bar{p} = r_0\omega/U$ where ω is the spin angular velocity. In the study a perturbation solution about $\alpha = \bar{p} = 0$ is used to solve the resulting boundary layer flow equations.

The boundary layer equations for incompressible laminar flow over the cylinder may be written (10) to order $(\delta/r_0)^2$ as

$$(ru)_x + (rv)_r + w_\varphi = 0 \tag{1}$$

$$uu_x + vu_r + \frac{wu_\varphi}{r} = \nu\left(u_{rr} + \frac{u_r}{r} + \frac{u_{\varphi\varphi}}{r^2}\right) \tag{2}$$

$$uw_x + vw_r + \frac{ww_\varphi}{r} + \frac{vw}{r} = -\frac{p_\varphi}{\rho r} + \nu\left(w_{rr} + \frac{w_r}{r} + \frac{w_{\varphi\varphi} - w}{r^2}\right) \tag{3}$$

where u, v, and w are the flow velocity components in the x, r, and φ directions respectively and the subscripts denote differentiation with respect to the coordinate direction. The axial pressure gradient p_x is of

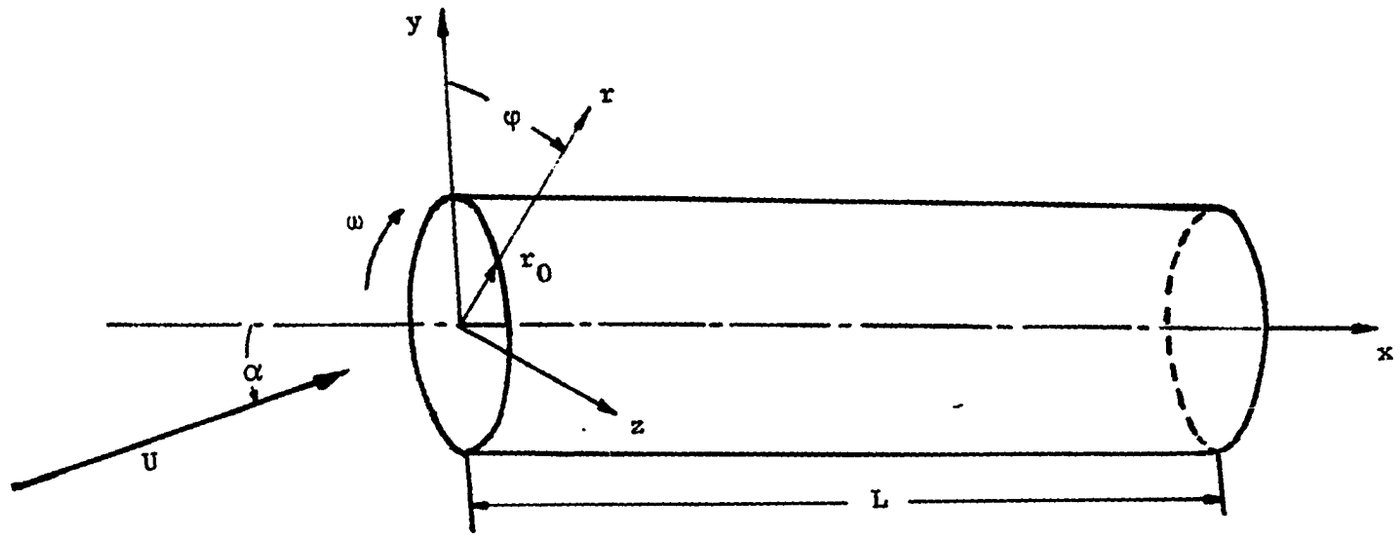

Figure 1a. Rotating cylinder

higher order than $(\delta/r_0)^2$ and, thus, is neglected. The radial pressure gradient p_r is of order $(\delta/L)^2$ so it is neglected when u, v, and w are calculated but the radial component of the momentum equation

$$uv_x + vv_r + \frac{wv_\varphi}{r} - \frac{w^2}{r} = -\frac{p_r}{\rho} + \frac{\nu}{r}(rv_r)_r \tag{4}$$

is used after u, v, and w are determined to calculate a correction of the previous solution due to the radial pressure gradient.

The boundary conditions at the cylinder surface are

$$\begin{aligned} u &= v = 0 \\ w &= \bar{p}U \end{aligned} \tag{5}$$

However, the conditions at the outer edge of the boundary layer require more discussion. Both Martin (14) and Kelly (10) assumed that no circulation was present in the inviscid outer flow. It has been established that there is indeed a circulation caused primarily by the eventual separation of the boundary layer, the resulting shed vorticity inducing an equal but opposite circulation in the outer flow. It is through this mechanism, at angles of attack sufficiently large for separation to occur, that the moving wall communicates its effects to the outer flow. It has been suggested by Buford (1) that the crossflow component of the flow over a spinning slender missile is similar to that about a rotating circular cylinder placed perpendicular to the freestream. If we assume this to be true, the crossflow along the x axis of a spinning cylinder at low angles of attack is similar to the unsteady solution of the flow over an impulsively rotated cylinder.

This leads to an axial circulation distribution for the spinning missile. For these reasons the boundary conditions at the outer edge were assumed to be similar to those of a slender body of revolution at an angle of attack when acted upon by the superposition of a uniform freestream velocity U and an axial irrotational vortex distribution $\Gamma(x)$. The resulting boundary conditions are

$$\begin{aligned} u &= U \cos \alpha \cong U\left(1 - \frac{\alpha^2}{2}\right) \\ w &\cong U \alpha \sin \varphi \left(1 + \frac{R_0^2}{r^2}\right) + \frac{k(x)\Gamma_0}{2\pi r} \end{aligned} \tag{6}$$

where $\Gamma_0 = 2\pi r_0 V$, $k(x)$ is the fraction of Γ_0 that corresponds to the inviscid circulation $\Gamma(x)$, and R_0 is the distance from the cylinder axis to the outer edge of the boundary layer.

In this investigation the solution of these boundary layer equations is carried out by a perturbation process suggested by Martin (14) and Kelly (10). The velocities are assumed to be in the form

$$\begin{aligned} \frac{u}{U} &= u_0 + u_1 + u_2 \\ \frac{v}{U} &= v_0 + v_1 + v_2 \\ \frac{w}{U} &= w_1 + w_2 \end{aligned} \tag{7}$$

where the subscript corresponds to the order of the perturbation quantities α and $\bar{p}$. For example, the 2 subscripted dimensionless velocities involve terms of order α^2, $\bar{p}^2$, and $\alpha\bar{p}$. Since, at $\alpha = 0$, u and v are even functions

of $\bar{p}$ and w is an odd function, u_1 and v_1 are independent of $\bar{p}$ and w_2 is independent of $\bar{p}^2$.

Substituting the assumed velocities into Equations 1 through 3, the zero order solution ($\alpha = \bar{p} = 0$) equations are

$$(ru_0)_x + (rv_0)_r = 0 \tag{8}$$

$$u_0 u_{0_x} + v_0 u_{0_r} = \frac{\nu}{Ur} (ru_{0_r})_r \tag{9}$$

where ν is the kinematic viscosity coefficient. Using the normal dimensionless boundary layer coordinates,

$$\xi = \frac{4}{r_0} \sqrt{\frac{\nu x}{U}} \tag{10}$$

$$\eta = \frac{r^2 - r_0^2}{4r_0} \sqrt{\frac{U}{\nu x}} \tag{11}$$

Equation 8 is satisfied when

$$u_0 = \frac{f_\eta}{2} \tag{12}$$

$$v_0 = \frac{r_0}{2r} \sqrt{\frac{\nu}{Ux}} (\eta f_\eta - f - \xi f_\xi) \tag{13}$$

where f is an unknown function of η and ξ. Equation 9 transforms to

$$[(1 + \eta\xi) f_{\eta\eta}]_\eta + f f_\eta + \xi [f_\xi f_{\eta\eta} - f_\eta f_{\eta\xi}] = 0 \tag{14}$$

To reduce Equation 14 to a system of ordinary differential equations we assume

$$f(\eta, \xi) = f_0(\eta) + \xi f_1(\eta) + \xi^2 f_2(\eta) \tag{15}$$

The resulting set of equations is

$$f_0''' = - f_0 f_0'' \tag{16}$$

$$f_1''' = f_0' f_1' - f_0 f_1'' - 2 f_0'' f_1 - \eta f_0''' - f_o'' \tag{17}$$

$$f_2''' = 2 f_0' f_2' - f_0 f_2'' - 3 f_0'' f_2 - \eta f_1''' - f_1'' - 2 f_1 f_1'' + f_1'^2 \tag{18}$$

with boundary conditions

$$\begin{aligned} f_0(0) &= f_0'(0) = 0 & f_0'(\infty) &= 2 \\ f_1(0) &= f_1'(0) = 0 & f_1'(\infty) &= 0 \\ f_2(0) &= f_2'(0) = 0 & f_2'(\infty) &= 0 \end{aligned} \tag{19}$$

For perturbations of order α and $\bar{p}$, Equations 1 through 3 become

$$(ru_1)_x + (rv_1)_r + w_{1_\varphi} = 0 \tag{20}$$

$$u_0 u_{1_x} + u_1 u_{0_x} + v_0 u_{1_r} + v_1 u_{0_r} + \frac{w_1 u_{1_\varphi}}{r} = \frac{\nu}{u}\left(u_{1_{rr}} + \frac{u_{1_r}}{r} + \frac{u_{1_{\varphi\varphi}}}{r^2}\right) \tag{21}$$

$$u_0 w_{1_x} + v_0 w_{1_r} + \frac{v_0 w_1}{r} = \frac{\nu}{U}\left(w_{1_{rr}} + \frac{w_{1_r}}{r} + \frac{w_{1_{\varphi\varphi}} - w_1}{r^2}\right) \tag{22}$$

Assuming

$$u_1 = \alpha\left(\frac{x}{r}\right) \cos \varphi \, K \tag{23}$$

$$v_1 = \alpha\left(\frac{x}{r_0}\right)\sqrt{\frac{\nu}{U_x}} \cos \varphi \, L \tag{24}$$

$$w_1 = \frac{\bar{p}}{2}\left(\frac{r_0}{r}\right)[2 - (1 - k)g] + \frac{\alpha}{2}\left(1 + \frac{R_0^2}{r^2}\right) \sin \varphi\, H \tag{25}$$

The transformed equations become

$$2K - \eta K_\eta + \xi K_\xi + (1 + \eta\xi)L_\eta + \frac{\xi}{2} L + \left(1 + \frac{R_0^2}{r^2}\right)H = 0 \tag{26}$$

$$(1 + \eta\xi)K_{\eta\eta} - f_\eta(2K - \eta K_\eta + \xi K_\xi) - (\xi f_{\eta\xi} - \eta f_{\eta\eta})K - (1 + \eta\xi) f_{\eta\eta} L$$
$$- (\eta f_\eta - f - \xi f_\xi)\left(K_\eta - \frac{\xi K}{2(1+\eta\xi)}\right) = 0 \tag{27}$$

$$f g_\eta + \xi f_\xi g_\eta - \xi f_\eta g_\xi + (1 + \eta\xi) g_{\eta\eta} + \frac{\xi f_\eta g k_\xi}{(1-k)} = 0 \tag{28}$$

$$(1 + \eta\xi) f_\eta(\xi H_\xi - \eta H_\eta)\left(1 + \frac{R_0^2}{r^2}\right) + (\eta f_\eta - f + \xi f_\xi + \xi)\left\{\frac{\xi}{2}\left(1 + \frac{R_0^2}{r^2}\right) H \right.$$
$$\left. + (1 + \eta\xi)\left(1 + \frac{R_0^2}{r^2}\right) H_\eta\right\} - (1 + \eta\xi)^2\left(1 + \frac{R_0^2}{r^2}\right) H_{\eta\eta}$$
$$- 2\xi(1 + \eta\xi) H_\eta = 0 \tag{29}$$

To reduce these equations to a set of ordinary differential equations the profile functions g, H, K, and L are expanded in a fashion similar to that used in the expansion of f. The resulting set of equations is, then,

$$L_0' = \eta K_0' - 2K_0 - 2H_0 \tag{30}$$

$$L_1' = - 3K_1 - \frac{L_0}{2} - 2H_1 - (.8604 - \eta)H_0 - \eta(L_0' - K_1') \tag{31}$$

$$L_2' = \eta K_2' - 4K_2 - \eta L_1' - \frac{1}{2} - 2H_2 - (.8604 - \eta)H_1 \tag{32}$$

$$K_0'' = f_0''(L_o - \eta K_0) + 2f_0' K_0 - f_0 K_0' \tag{33}$$

$$K_1'' = -\eta K_0'' + f_0''(L_1 + \eta L_0 - \eta K_1) + f_0'(3K_1 - \frac{\eta K_0}{2})$$

$$+ f_0(\frac{K_0}{2} - K_1') - 2f_1K_0' + 3f_1'K_0 + f_1''(L_0 - \eta K_0) \qquad (34)$$

$$K_2'' = -2\eta K_1'' - \eta^2 K_0'' - f_0K_2' + f_0''L_2 + K_2(4f_0' - \eta f_0'')$$

$$- K_1'(2f_1 + \eta f_0) + K_1(4f_1' - \eta f_1'' + \frac{5\eta f_0'}{2} - \eta^2 f_0'' + \frac{f_0}{2})$$

$$- K_0'(3f_2 + 2\eta f_1) + K_0(4f_2' - \eta f_2'' + \frac{5\eta f_1'}{2} - \eta^2 f_1'' + f_1)$$

$$+ L_1(f_1'' + 2\eta f_0'') + L_0(f_2 + 2\eta f_1'' + \eta^2 f_0'') \qquad (35)$$

$$g_0'' = - f_0g_0' \qquad (36)$$

$$g_1'' = f_0'g_1 - f_0g_1' - 2f_1g_0' - \eta g_0'' \qquad (37)$$

$$g_2'' = 2f_0'g_2 + f_1'g_1 - f_0g_2' - 2f_1g_1' - 3f_2g_0' - \eta g_0''$$

$$- \frac{k_\xi}{\xi(1-k)} f_0'g_0 \qquad (38)$$

$$H_0'' = - f_0H_0' \qquad (39)$$

$$H_1'' = f_0'H_1 - f_0H_1' - H_0'\left\{2f_1 + \frac{(.8604 + \eta)}{2} f_0\right\}$$

$$- \frac{(.8604 + 3\eta)}{2} H_0'' \qquad (40)$$

$$H_2'' = 2f_0'H_2 - f_0H_2' - .8604\eta H_0'' - \frac{(.8604 + 3\eta)}{2} H_1''$$

$$+ H_1\left\{f_1' + \frac{(.8604 + \eta)}{2} f_0'\right\} - H_1'\left\{\frac{(.8604 + \eta)}{2} f_0 + 2f_1\right\}$$

$$+ H_0' \left\{ \frac{(.8604 - \eta)}{2} - 3f_2 - (.8604 + \eta) f_1 - \frac{(.8604 - \eta)}{2} \eta f_0 \right\}$$

$$- H_0 (\eta f_0' - f_0) \left(\frac{.8604 - \eta}{4} \right) \tag{41}$$

with boundary conditions

$$\begin{aligned}
&g_0(0) = g_1(0) = g_2(0) = 0 \\
&H_0(0) = H_1(0) = H_2(0) = 0 \\
&K_0(0) = K_1(0) = K_2(0) = 0 \\
&L_0(0) = L_1(0) = L_2(0) = 0 \\
&g_0(\infty) = H_0(\infty) = 2 \\
&g_1(\infty) = g_2(\infty) = 0 \\
&H_1(\infty) = H_2(\infty) = 0 \\
&K_0(\infty) = K_1(\infty) = K_2(\infty) = 0
\end{aligned} \tag{42}$$

It may be noticed that

$$g_0 = H_0 = f_0' \tag{43}$$

from Equations 36 and 39.

Equations 1 through 3 for perturbations of order α^2, $\alpha\bar{p}$, and $\bar{p}^2$ become

$$(ru_2)_x + (rv_2)_r + w_{2_\varphi} = 0 \tag{44}$$

$$u_0 u_{2_x} + u_1 u_{1_x} + u_2 u_{0_x} + v_0 u_{2_r} + v_1 u_{1_r} + \frac{w_1 u_{1_\varphi}}{r}$$

$$= \frac{\nu}{U}\left(u_{2_{rr}} + \frac{u_{2_r}}{r} + \frac{u_{2_{\varphi\varphi}}}{r^2}\right) \tag{45}$$

$$u_0 w_{2_x} + u_1 w_{1_x} + v_0 w_{2_r} + v_1 w_{1_r} + \frac{w_1 w_{1_\varphi}}{r} + \frac{v_0 w_2}{r} + \frac{v_1 w_1}{r}$$

$$= \frac{\nu}{U}\left(w_{2_{rr}} + \frac{w_{2_r}}{r} + \frac{w_{2_{\varphi\varphi}} - w_2}{r^2}\right) + \frac{4\alpha^2 r_0^2}{r^2} \sin\varphi \cos\varphi$$

$$+ \frac{2\cos\varphi}{r}\left(1 + \frac{r_0^2}{r^2}\right)\alpha\bar{p} \tag{46}$$

where the last two terms of Equation 46 are the slender body pressure gradient terms in the φ direction. If we assume

$$u_2 + \left(\frac{x}{r}\right)^2 \alpha\bar{p} \sin\varphi\, P + \left(\frac{x}{r}\right)^2 \alpha^2 (Q + T\cos 2\varphi) - \frac{\alpha^2}{2} z_\eta + \frac{\bar{p}^2}{2}\lambda_\eta \tag{47}$$

$$v_2 = \frac{x^2}{rr_0}\sqrt{\frac{\nu}{Ux}}\,\alpha\bar{p} \sin\varphi\beta + \frac{x^2}{rr_0}\sqrt{\frac{\nu}{Ux}}\,\alpha^2(\gamma + \epsilon\cos 2\varphi)$$

$$- \frac{r_0}{2r}\sqrt{\frac{\nu}{Ux}}\,\alpha^2(\eta z_\eta - z - \xi z_\xi) + \frac{r_0}{2r}\sqrt{\frac{\nu}{Ux}}\,\bar{p}^2(\eta\lambda_\eta - \lambda - \xi\lambda_\xi) \tag{48}$$

$$w_2 = \left(\frac{x}{r}\right)\alpha\bar{p}\cos\varphi\, M + \left(\frac{x}{r}\right)\alpha^2 \frac{\sin 2\varphi}{2} N \tag{49}$$

Transformation of the equations results in

$$\xi P_\xi - \eta P_\eta + 4P + (1 + \eta\xi)\beta_\eta - 2M = 0 \tag{50}$$

$$\xi T_\xi - \eta T_\eta + 4T + (1 + \eta\xi)\epsilon_\eta + 2N = 0 \tag{51}$$

$$\xi Q_\xi - \eta Q_\eta + 4Q + (1 + \eta\xi)\gamma_\eta = 0 \tag{52}$$

$$\xi f_\eta \lambda_{\eta\xi} + \xi f_{\eta\xi} \lambda_\eta - (f + \xi f_\xi + \frac{\xi}{2}) \lambda_{\eta\eta} - f_{\eta\eta}(\lambda + \xi \lambda_\xi)$$

$$- (1 + \eta\xi) \lambda_{\eta\eta\eta} = 0 \tag{53}$$

$$\xi f_\eta z_{\eta\xi} + \xi f_{\eta\xi} z_\eta - (f + \xi f_\xi + \xi) z_{\eta\eta} - f_{\eta\eta}(z + \xi z_\xi)$$

$$- (1 + \eta\xi) z_{\eta\eta\eta} = 0 \tag{54}$$

$$P \left\{ 4f_\eta + \xi f_{\eta\xi} - \eta f_{\eta\eta} - \frac{\xi}{(1 + \eta\xi)} (\eta f_\eta - f - \xi f_\xi) - \frac{3\xi^2}{4(1 + \eta\xi)} \right\}$$

$$+ \xi f_\eta P_\xi + P_\eta (\xi - f - \xi f_\xi) - (1 + \eta\xi) P_{\eta\eta} + (1 + \eta\xi) f_{\eta\eta} \beta$$

$$- \frac{2K}{\sqrt{1 + \eta\xi}} \left\{ 2 - (1 - k) g \right\} = 0 \tag{55}$$

$$T \left\{ 4f_\eta + \xi f_{\eta\xi} - \eta f_{\eta\eta} - \frac{\xi}{(1 + \eta\xi)} (\eta f_\eta - f - \xi f_\xi) \right\} + \xi f_\eta T_\xi$$

$$+ T_\eta (\xi - f - \xi f_\xi) - (1 + \eta\xi) T_{\eta\eta} + (1 + \eta\xi) f_{\eta\eta} \varepsilon + (1 + \eta\xi) K_\eta L$$

$$+ K \left\{ 2K - \eta K_\eta + \xi K_\xi - \frac{\xi}{2} L + (1 + \frac{R_0^2}{r^2}) H \right\} = 0 \tag{56}$$

$$Q \left\{ 4f_\eta + \xi f_{\eta\xi} - \eta f_{\eta\eta} - \frac{\xi}{(1 + \eta\xi)} (\eta f_\eta - f - \xi f_\xi) - \frac{\xi^2}{(1 + \eta\xi)} \right\}$$

$$+ \xi f_\eta Q_\xi + Q_\eta (\xi - f - \xi f_\xi) - (1 + \eta\xi) Q_{\eta\eta} + (1 + \eta\xi) f_{\eta\eta} \gamma$$

$$+ (1 + \eta\xi) K_\eta L + K \left\{ 2K - \eta K_\eta + \xi K_\xi - \frac{\xi}{2} L - (1 + \frac{R_0^2}{r^2}) H \right\} = 0$$

(57)

$$N(2f_\eta + \frac{\xi^2}{(1 + \eta\xi)}) + \xi f_\eta N_\xi + N_\eta (-f - \xi f_\xi) - (1 + \eta\xi) N_{\eta\eta} - 16 (\frac{R_0}{r})^2$$

$$+ (1 + \frac{R_0^2}{r^2}) \left\{ (1 + \frac{R_0^2}{r^2}) H^2 + K(\xi H_\xi - \eta H_\eta) + (1 + \eta\xi) L H_\eta \right\}$$

$$+ \left(1 - \frac{R_0^2}{r^2}\right) \frac{\xi}{2} HL = 0 \tag{58}$$

$$M\left(2f_\eta + \frac{\xi^2}{4(1+\eta\xi)}\right) + \xi f_\eta M_\xi + M_\eta(-f - \xi f_\xi) - (1+\eta\xi)M_{\eta\eta}$$

$$- \frac{(1-k)}{\sqrt{1+\eta\xi}} K(\xi g_\xi - \eta g_\eta) - (1-k)(1+\eta\xi)^{\frac{1}{2}} L g_\eta$$

$$+ \frac{\xi}{\sqrt{1+\xi\eta}} K g k_\xi + \left(1 + \frac{R_0^2}{r^2}\right)\left\{\frac{[2-(1-k)g]}{\sqrt{1+\eta\xi}} H - 4k\right\} = 0 \tag{59}$$

Reducing this set of equations to a set of ordinary ones we get

$$\beta_0' = 2M_0 - 4P_0 + \eta P_0' \tag{60}$$

$$\beta_1' = 2M_1 + \eta P_1' - 5P_1 - \eta\beta_0' \tag{61}$$

$$\beta_2' = 2M_2 + \eta P_2' - 6P_2 - \eta\beta_1' \tag{62}$$

$$\epsilon_0' = 2N_0 - 4T_0 + \eta T_0' \tag{63}$$

$$\epsilon_1' = 2N_1 + \eta T_1' - 5T_1 - \eta\epsilon_0' \tag{64}$$

$$\epsilon_2' = 2N_2 + \eta T_2' - 6T_2 - \eta\epsilon_1' \tag{65}$$

$$\gamma_0' = \eta Q_0' - 4Q_0 \tag{66}$$

$$\gamma_1' = \eta Q_1' - 5Q_1 - \eta\gamma_0' \tag{67}$$

$$\gamma_2' = \eta Q_2' - 6Q_2 - \eta\gamma_1' \tag{68}$$

$$\lambda_0''' = -f_0\lambda_0'' - f_0''\lambda_0 \tag{69}$$

$$\lambda_1''' = -f_1''\lambda_0 + f_1'\lambda_0' - \lambda_0''(2f_1 + \tfrac{1}{2}) - \eta\lambda_0'' - 2f_0''\lambda_1$$

$$+ f_0'\lambda_1' - f_0\lambda_1'' \tag{70}$$

$$\lambda_2''' = -\eta\lambda_1''' + 2f_0'\lambda_2' + 2f_1'\lambda_1' + 2f_2'\lambda_0' - f_0\lambda_2''$$

$$- \lambda_1''(2f_1 + \tfrac{1}{2}) - 3f_2\lambda_0'' - 3f_0''\lambda_2 - 2f_1''\lambda_1 - f_2''\lambda_0 \tag{71}$$

$$z_0''' = -f_0z_0'' - f_0''z_0 \tag{72}$$

$$z_1''' = -f_1''z_0 + f_1'z_0' - z_0''(2f_1 + 1) - \eta z_0''' - 2f_0''z_1$$

$$+ f_0'z_1' - f_0z_1'' \tag{73}$$

$$z_2''' = -\eta z_1''' + 2f_0'z_2' + 2f_1'z_1' + 2f_2'z_0' - f_0z_2''$$

$$- z_1''(2f_1 + 1) - 3f_2z_0'' - 3f_0''z_2 - 2f_1''z_1 - f_2''z_0 \tag{74}$$

$$P_0'' = \beta_0 f_0'' + P_0(4f_0' - \eta f_0'') - f_0P_0' - 4K_0 + 2K_0g_0 \tag{75}$$

$$P_1'' = -2\eta P_0'' + P_0'(1 - 2f_1 - \eta f_0) + P_1(4f_0 - \eta f_0'' + f_0') - f_0P_1'$$

$$- 4K_1 + P_0(3\eta f_0' - \eta^2 f_0'' + f_0 + 5f_1' - \eta f_1'') + \beta_1 f_0''$$

$$+ \beta_0(f_1'' + 2\eta f_0'') + 2(K_0g_1 - K_1g_0 - \eta K_0 + \frac{\eta}{2} K_0g_0) \tag{76}$$

$$P_2'' = -2\eta P_1'' - \eta^2 P_0'' - f_0P_2' + P_1'(1 - 2f_1 - \eta f_0) + P_2(6f_0' - \eta f_0)$$

$$+ P_0'(\eta - 3f_2 - \eta f_1 - \eta^2 f_0) + P_1(f_0 + 4\eta f_0' - \eta^2 f_0''$$

$$+ 6f_1' - \eta f_1'') + P_0(2f_1 - \frac{3}{4} + 4\eta f_1' - \eta^2 f_1'' + 6f_2' - \eta f_2'')$$

$$- 4K_2 - 2\eta K_1 + \frac{\eta^2}{2} K_0 + \beta_0(f_2'' + 2\eta f_1'' + 5\eta^2 f_0'')$$

$$+ \beta_1(f_1'' + 2\eta f_0'') + \beta_2 f_0'' + 2K_0\left(g_2 + \frac{\eta}{2} g_1 - \frac{\eta^2}{8} g_0\right)$$

$$+ 2K_1\left(g_1 + \frac{\eta}{2} g_0\right) + 2K_2 g_0 - \frac{2k}{\xi^2} K_0 g_0 \tag{77}$$

$$T_0'' = \epsilon_0 f_0'' + T_0(4f_0' - \eta f_0'') - f_0 T_0' + 2K_0^2 - \eta K_0 K_0'$$

$$+ 2K_0 H_0 + L_0 K_0' \tag{78}$$

$$T_1'' = -2\eta T_0'' + T_0'(1 - 2f_1 - \eta f_0) + T_1(4f_0 + f_0' - \eta f_0'')$$

$$- f_0 T_1' + T_0(3\eta f_0' - \eta^2 f_0'' + f_0 + 5f_1' - \eta f_1'') + \epsilon_1 f_0''$$

$$+ \epsilon_0(f_1'' + 2\eta f_0'') + K_1(5K_0 - \eta K_0' + 2H_0) + K_1'(L_0 - \eta K_0)$$

$$+ K_0\left[2H - \frac{L_0}{2} + 2\eta K_0 + (.8604 + \eta) H_0\right] + K_0'(L_1 + 2\eta L_0 - \eta^2 K_0)$$

(79)

$$T_2'' = -2\eta T_1'' - \eta^2 T_0'' + T_1'(1 - 2f_1 - \eta f_0) - f_0 T_2'$$

$$+ T_0'(\eta - 3f_2 - \eta f_1 - \eta^2 f_0) + T_2(6f_0' - \eta f_0'')$$

$$+ T_1(f_0 + 4\eta f_0' - \eta^2 f_0'' + 6f_1' - \eta f_1'') + T_0(2f_1 + 4\eta f_1'$$

$$- \eta^2 f_1'' + 6f_2' - \eta f_2'') + \epsilon_0(f_2'' + 2\eta f_1'' + 5\eta^2 f_0'')$$

$$+ \epsilon_1(f_1'' + 2\eta f_0'') + \epsilon_2 f_0'' + K_2'(L_0 - \eta K_0)$$

$$+ K_2(6K_0 + 2H_0 - \eta K_0') + K_1'(L_1 + 2\eta L_0 - \eta K_1 - \eta^2 K_0)$$

$$+ K_1\left(3K_1 + 2H_1 - \frac{L_0}{2} + 5\eta K_0 + 2\eta H_0 - \eta^2 K_0'\right)$$

$$+ K_0'(L_2 + 2\eta L_1 + \eta^2 L_0) + (.8604 - \eta)(K_0 H_0 + K_1 H_0 + K_0 H_1)$$

$$+ K_0(2H_2 + 2\eta H_1 - \frac{\eta L_0}{2} - \frac{L_1}{2}) \tag{80}$$

$$Q_0'' = \gamma_0 f_0'' + Q_0(4f_0' - \eta f_0'') - f_0 Q_0' + 2K_0^2 - \eta K_0 K_0'$$

$$- 2K_0 H_0 + L_0 K_0' \tag{81}$$

$$Q_1'' = -2\eta Q_0'' + Q_0'(1 - 2f_1 - \eta f_0) + Q_1(4f_0 + f_0' - \eta f_0'')$$

$$- f_0 Q_1' + Q_0(3\eta f_0' - \eta^2 f_0'' + f_0 + 5f_1' - \eta f_1'') + \gamma_1 f_0''$$

$$+ \gamma_0(f_1'' + 2\eta f_0'') + K_1(5K_0 - \eta K_0' - 2H_0) + K_1'(L_0 - \eta K_0)$$

$$+ K_0'(L_1 + 2\eta L_0 - \eta^2 K_0) + K_0[2\eta K_0 - 2H_1 - \frac{L_0}{2} - (.8604 + \eta)H_0]$$

(82)

$$Q_2'' = -2\eta Q_1'' - \eta^2 Q_0'' + Q_1'(1 - 2f_1 - \eta f_0) - f_0 Q_2'$$

$$+ Q_2(6f_0' - \eta f_0'') + Q_0'(\eta - 3f_2 - \eta f_1 - \eta^2 f_0)$$

$$+ Q_1(f_0 + 4\eta f_0' - \eta^2 f_0'' + 6f_1' - \eta f_1'')$$

$$+ Q_0(1 + 2f_1 + 4\eta f_1' - \eta^2 f_1'' + 6f_2' - \eta f_2'')$$

$$+ \gamma_0(f_2'' + 2\eta f_1'' + 5\eta^2 f_0'') + \gamma_1(f_1'' + 2\eta f_0'') + \gamma_2 f_0''$$

$$+ K_2'(L_0 - \eta K_0) + K_2(6K_0 - 2H_0 - \eta K_0')$$

$$+ K_1'(L_1 + 2\eta L_0 - \eta K_1 - \eta^2 K_0) + K_1(3K_1 - 2H_1 - \frac{L_0}{2} + 5\eta K_0$$

$$- 2\eta H_0 - \eta^2 K_0') + K_0'(L_2 + 2\eta L_1 + \eta^2 L_0)$$

$$- (.8604 - \eta)(K_1 H_0 + K_0 H_1 + H_0 K_0) \tag{83}$$

$$N_0'' = 2f_0' N_0 - f_0 N_0' - 16 - 2\eta H_0' + 2L_0 H_0' + 4H_0^2 \tag{84}$$

$$N_1'' = -2\eta N_0'' + N_0(2f_1' + 2\eta f_0') + N_0'(-\eta f_0 - 2f_1) + 3f_0'N_1$$
$$- f_0N_1' - 13.7664 + 3.4416\,H_0^2 + H_1(8H_0 + 2K_0)$$
$$+ 2H_1'(L_0 - \eta K_0) + 2H_0'(L_1 + \eta L_0 - \eta K_1)$$
$$+ (.8604 - \eta)(L_0H_0' - \eta K_0H_0') \qquad (85)$$

$$N_2'' = -2\eta N_1'' - \eta^2 N_0'' - N_1'(2f_1 + \eta f_0) + f_0N_2' + 4f_0'N_2$$
$$- N_0'(3f_2 + 2\eta f_1) + 3N_1(f_1 + \eta f_0') + N_0(1 + 2f_2' + 2\eta f_1')$$
$$+ (.8604 - \eta)\eta - 2H_2'(L_0 + \eta K_0) + 4K_0H_2$$
$$+ H_1'[2L_1 + 2\eta L_0 - 2\eta K_1 + (.8604 + \eta)(L_0 - \eta K_0)]$$
$$+ H_0'[2L_2 + 2\eta L_1 - 2\eta K_2 + (.8604 + \eta)(L_1 + \eta L_0 - \eta K_1)$$
$$- \eta^2(.8604 - \eta)K_0] + H_1[4H_1 + K_1 + 2(.8604 - \eta)H_0$$
$$+ (.8604 + \eta)(4H_0 + K_0)] + H_0^2[.7403 + 1.7208\eta - 3\eta^2]$$
$$- \frac{H_0L_0}{2}(.8604 - \eta) \qquad (86)$$

$$M_0'' = 2f_0'M_0 - f_0M_0' + 4H_0 + \eta K_0g_0' - 2g_0H_0 - L_0g_0' \qquad (87)$$

$$M_1'' = -2\eta M_0'' + M_0(2f_1 + 2\eta f_0') - M_0'(\eta f_0 + 2f_1) + 3f_0'M_1$$
$$- f_0M_1' + 4H_1 + 1.7208\,H_0 - K_0g_1 + \eta K_0g_1' + \eta g_0'K_1$$
$$+ \frac{\eta^2}{2}K_0g_0' - 2g_0H_1 - 2g_1H_0 - .8604\,g_0H_0 - L_0g_1' - L_1g_0'$$
$$- \frac{3}{2}\eta L_0g_0' \qquad (88)$$

$$M_2'' = -2\eta M_1'' - \eta^2 M_0'' + f_0 M_2' + 4f_0' M_2 - M_1'(2f_1 + \eta f_0)$$

$$+ 3M_1(f_1' + \eta f_0') - M_0'(3f_2 - 2\eta f_1) + M_0(\tfrac{1}{4} + 2f_2' + 2\eta f_1')$$

$$+ 4H_2 + 1.7208\, H_1 + (.8604 - \frac{3\eta}{2})\,\eta H_0 - 2K_0 g_2$$

$$- g_2'(L_0 - \eta K_0) - g_1'(L_1 - \eta K_1 - \frac{\eta^2}{2} K_0 + \frac{3\eta}{2} L_0)$$

$$- g_1(K_1 + \frac{\eta}{2} K_0 + 2H_1 + 2.8604\, H_0)$$

$$- g_0'(\eta K_2 + \frac{\eta^2}{8} K_0 + L_2 + \frac{3\eta}{2} L_1 + \frac{3\eta^2}{8} L_0)$$

$$- g_0[2H_2 - \frac{\eta^2}{2} K_1' + .8604\, H_1 - \frac{\eta}{2}(.8604 - \frac{3\eta}{2})\, H_0]$$

$$- \frac{k}{\xi^2}(\eta K_0 g_0' - 2g_0 H_0 - L_0 g_0' + 8) + \frac{k_\xi}{\xi} K_0 g_0 \qquad (89)$$

Then the boundary conditions become

$$\beta_0(0) = \beta_1(0) = \beta_2(0) = 0$$

$$\epsilon_0(0) = \epsilon_1(0) = \epsilon_2(0) = 0$$

$$\gamma_0(0) = \gamma_1(0) = \gamma_2(0) = 0$$

$$\lambda_0(0) = \lambda_1(0) = \lambda_2(0) = 0$$

$$\lambda_0'(0) = \lambda_1'(0) = \lambda_2'(0) = 0$$

$$z_0(0) = z_1(0) = z_2(0) = 0$$

$$z_0'(0) = z_1'(0) = z_2'(0) = 0$$

$$P_0(0) = P_1(0) = P_2(0) = 0$$

$$Q_0(0) = Q_1(0) = Q_2(0) = 0$$

$$T_0(0) = T_1(0) = T_2(0) = 0 \qquad (90)$$

$$M_0(0) = M_1(0) = M_2(0) = 0$$

$$N_0(0) = N_1(0) = N_2(0) = 0$$

$$\lambda_0'(\infty) = \lambda_1'(\infty) = \lambda_2'(\infty) = 0$$

$$z_0'(\infty) = 1$$

$$z_1'(\infty) = z_2'(\infty) = 0$$

$$P_0(\infty) = P_1(\infty) = P_2(\infty) = 0$$

$$Q_0(\infty) = Q_1(\infty) = Q_2(\infty) = 0$$

$$T_0(\infty) = T_1(\infty) = T_2(\infty) = 0$$

$$M_0(\infty) = M_1(\infty) = M_2(\infty) = 0$$

$$N_0(\infty) = N_1(\infty) = N_2(\infty) = 0$$

The preceding equations of motion and boundary conditions are sufficient to determine the boundary layer velocity profiles if the circulation distribution k(x) is known. The two-dimensional numerical analysis of an impulsively rotated cylinder immersed in a uniform freestream as predicted by Thoman and Szewczyk (22) indicates that the cylinder lift coefficient is given by:

$$C_L = f\left(\frac{V}{U_\infty}\right)\left\{1 - e^{-\frac{.6U_\infty t}{d}\Big/\sqrt[4]{\frac{Ud}{\nu}}}\right\} \qquad (91)$$

where V is the surface speed of the cylinder and f is an unknown function of V/U_∞. To apply this result to the spinning cylinder crossflow we let

$$U_\infty = U \sin \alpha$$

$$t = \frac{x}{U \cos \alpha} \tag{92}$$

$$\frac{V}{U_\infty} = \frac{\bar{p}}{\sin \alpha}$$

Since the local circulation strength is given by

$$\Gamma = \tfrac{1}{2} C_L U_\infty d \tag{93}$$

we find that

$$k = \frac{\Gamma}{\Gamma_0} = \frac{1}{2\pi} \frac{\sin \alpha}{\bar{p}} f\left(\frac{\bar{p}}{\sin \alpha}\right) \left\{ 1 - e^{- \frac{.6 \, x \tan \alpha}{d} \Big/ \sqrt[4]{\frac{U \sin \alpha \, d}{\nu}}} \right\} \tag{94}$$

Assuming small α and transforming x to the dimensionless coordinate we find that

$$k \cong \frac{.6}{128 \, \pi} \left(\frac{\alpha}{\bar{p}}\right) f \left(\frac{\bar{p}}{\sin \alpha}\right) R_C^{3/4} \, \xi^2 \tag{95}$$

where R_C is the crossflow Reynolds number based on the cylinder diameter.

$$R_C = \frac{U d \alpha}{\nu} \tag{96}$$

Figure 1b shows the function f. This function was estimated by a curve fit of rotating cylinder data (8). We see that the circulation is of order ξ^2 for reasonable crossflow Reynolds numbers. In particular, for $\bar{p}/\sin \alpha \leqq 0.25$ we find

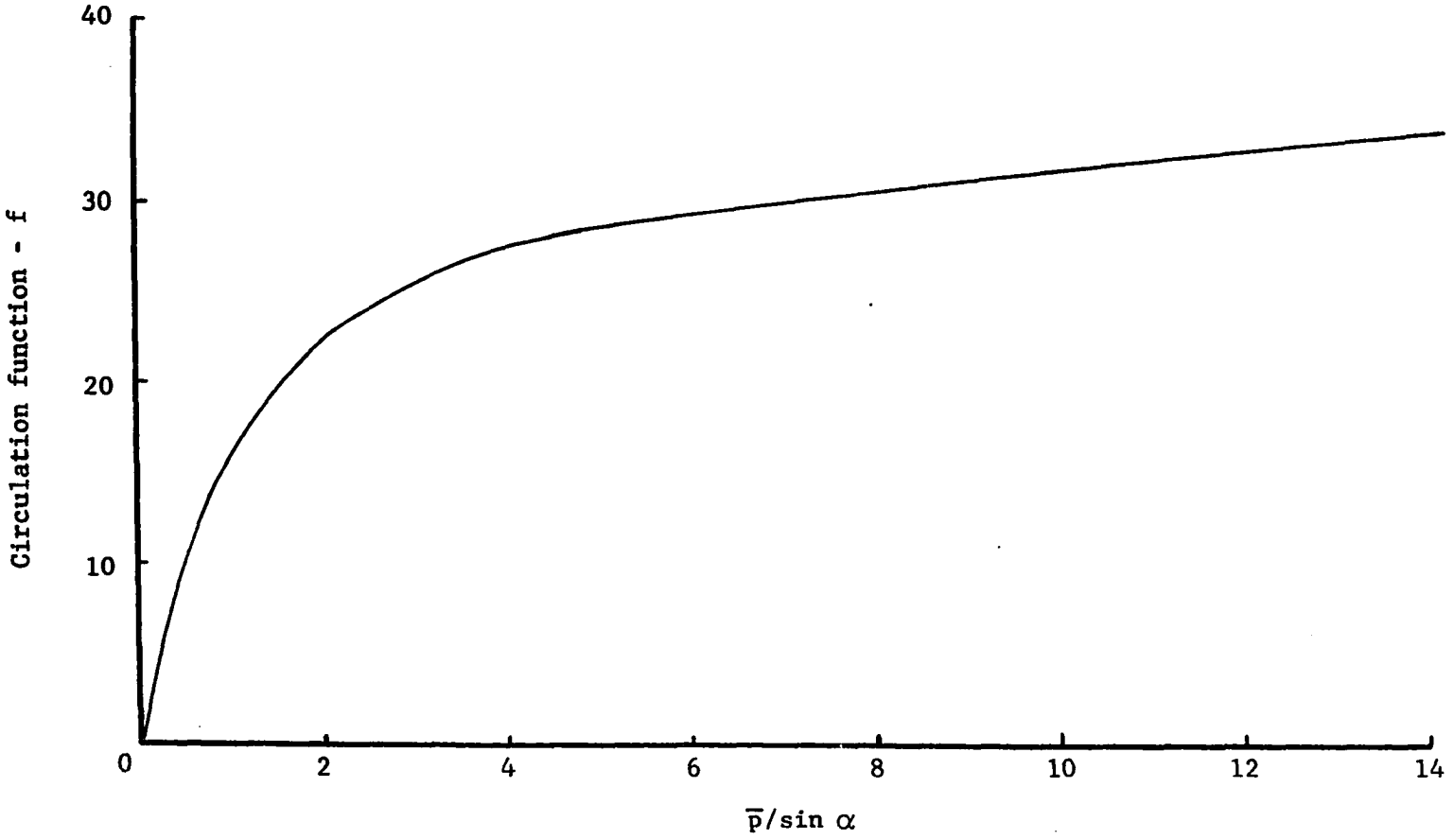

Figure 1b. Circulation function for spinning cylinders

$$f = 22 \frac{\bar{p}}{\sin \alpha} \tag{97}$$

which leads to a circulation distribution

$$k = .0328 R_C^{3/4} \xi^2 \tag{98}$$

If, on the other hand, $\bar{p}/\sin \alpha \cong 7.0$ we find that

$$f = .5278 \frac{\bar{p}}{\sin \alpha} + 26.406 \tag{99}$$

so that

$$k = .0015(.5278 + 26.406 \frac{\alpha}{\bar{p}}) R_C^{3/4} \xi^2 \tag{100}$$

Profile Functions

The formulation of the equations of motion has led to the following results for the boundary layer velocity profiles:

$$\frac{u}{U} = \frac{f_\eta}{2} + \alpha(\frac{x}{r}) \cos \varphi K + (\frac{x}{r})^2 \alpha \bar{p} \sin \varphi P + (\frac{x}{r})^2 (Q + T \cos 2\varphi)\alpha^2$$

$$- \frac{\alpha^2}{2} z_\eta + \frac{\bar{p}^2}{2} \lambda_\eta \tag{101}$$

$$\frac{v}{U} = \frac{r_0}{2r} \sqrt{\frac{\nu}{U_x}} (\eta f_\eta - f - \xi f_\xi) + \alpha(\frac{x}{r_0}) \sqrt{\frac{\nu}{U_x}} \cos \varphi L$$

$$+ \frac{x^2}{rr_0} \sqrt{\frac{\nu}{U_x}} \alpha \bar{p} \sin \varphi \beta + \frac{x^2}{rr_0} \sqrt{\frac{\nu}{U_x}} \alpha^2 (\gamma + \epsilon \cos 2\varphi)$$

$$- \frac{r_0}{2r} \sqrt{\frac{\nu}{U_x}} \alpha^2 (\eta z_\eta - z - \xi z_\xi) + \frac{r_0}{2r} \sqrt{\frac{\nu}{U_x}} \bar{p}^2 (\eta \lambda_\eta - \lambda - \xi \lambda_\xi) \tag{102}$$

$$\frac{w}{U} = \frac{\bar{p}}{2}(\frac{r_0}{r}) \left\{ 2 - (1 - k) g \right\} + \frac{\alpha}{2}(1 + \frac{R_0^2}{r^2}) \sin \varphi H + (\frac{x}{r}) \alpha \bar{p} \cos \varphi M$$

$$+ \left(\frac{x}{r}\right) \frac{\alpha^2}{r} \sin 2\varphi \, N \tag{103}$$

The profile function Equations 16 through 19, 30 through 43, and 60 through 90 were solved numerically by digital computer using the Iowa State University computer package DNODE. DNODE solves a system of first order differential equations using the predictor-corrector equations of R. L. Crane (2). The program integrates equations as an initial value problem. The equations of motion for the rotating cylinder are, however, of the two-point boundary value type. For this reason guesses of the unknown initial values are made and then the differential equations are integrated from the cylinder surface to the edge of the boundary layer. If the results are not satisfactory, the initial values are adjusted and the integration is repeated. This process is continued until the solutions satisfy the outer edge boundary conditions.

Figures 2 through 12 show the result of these calculations. In some cases difficulties prevented the calculation of the profile functions of order ξ^2. In fact, it was found that it was necessary to guess the initial values for some of these highest order profile functions very accurately before the numerical solution converged to the correct value for large values of the independent variable η. It should be noted that the profile functions of order ξ^2 are dependent upon the previous profile function solutions of lower order. For this reason it is likely that some of the numerical instability encountered is due to roundoff errors.

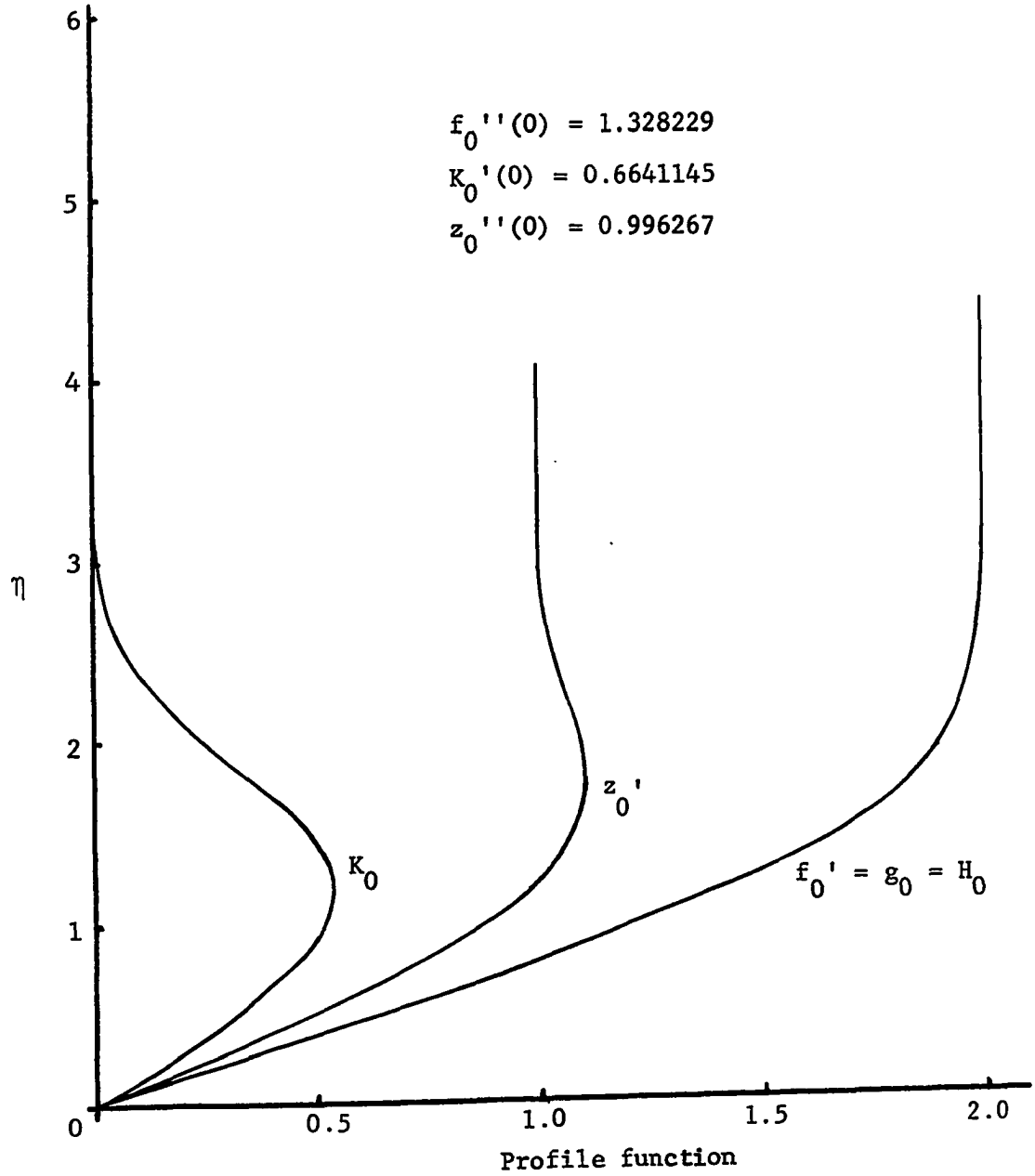

Figure 2. Velocity profile functions f_0', g_0, H_0, K_0 and z_0' for a spinning cylinder

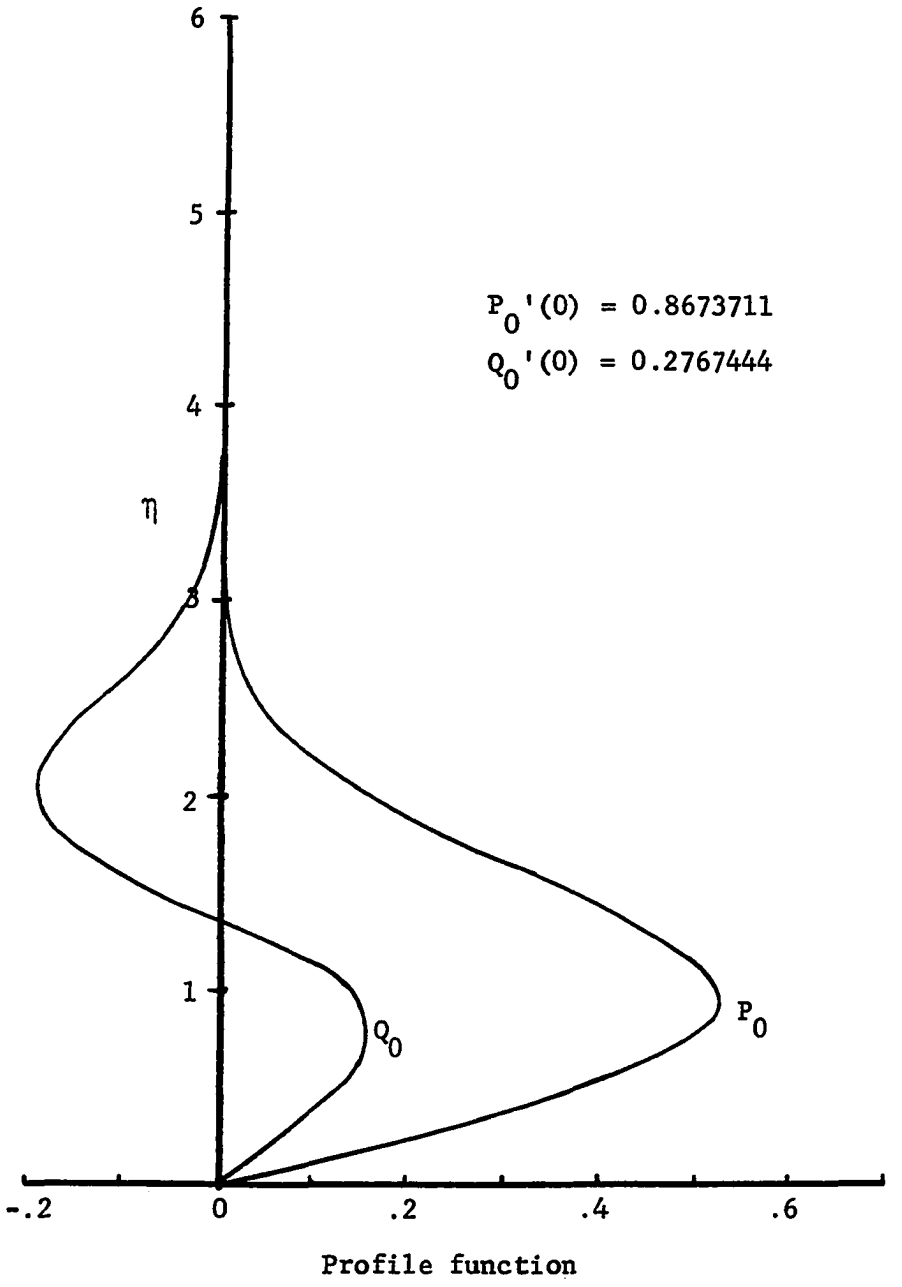

Figure 3. Velocity profile functions P_0 and Q_0 for a spinning cylinder

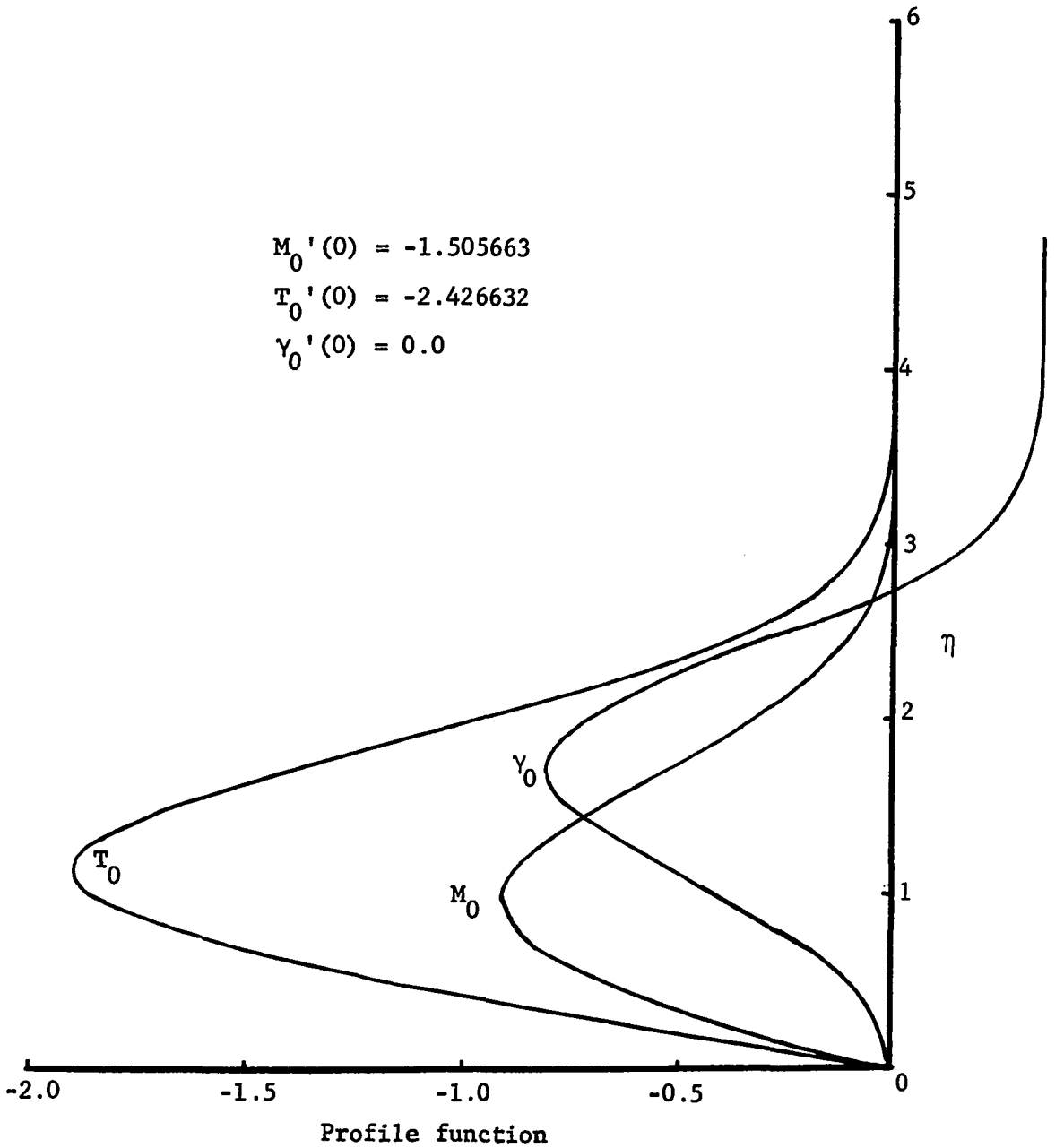

Figure 4. Profile functions M_0, T_0 and γ_0 for a spinning cylinder

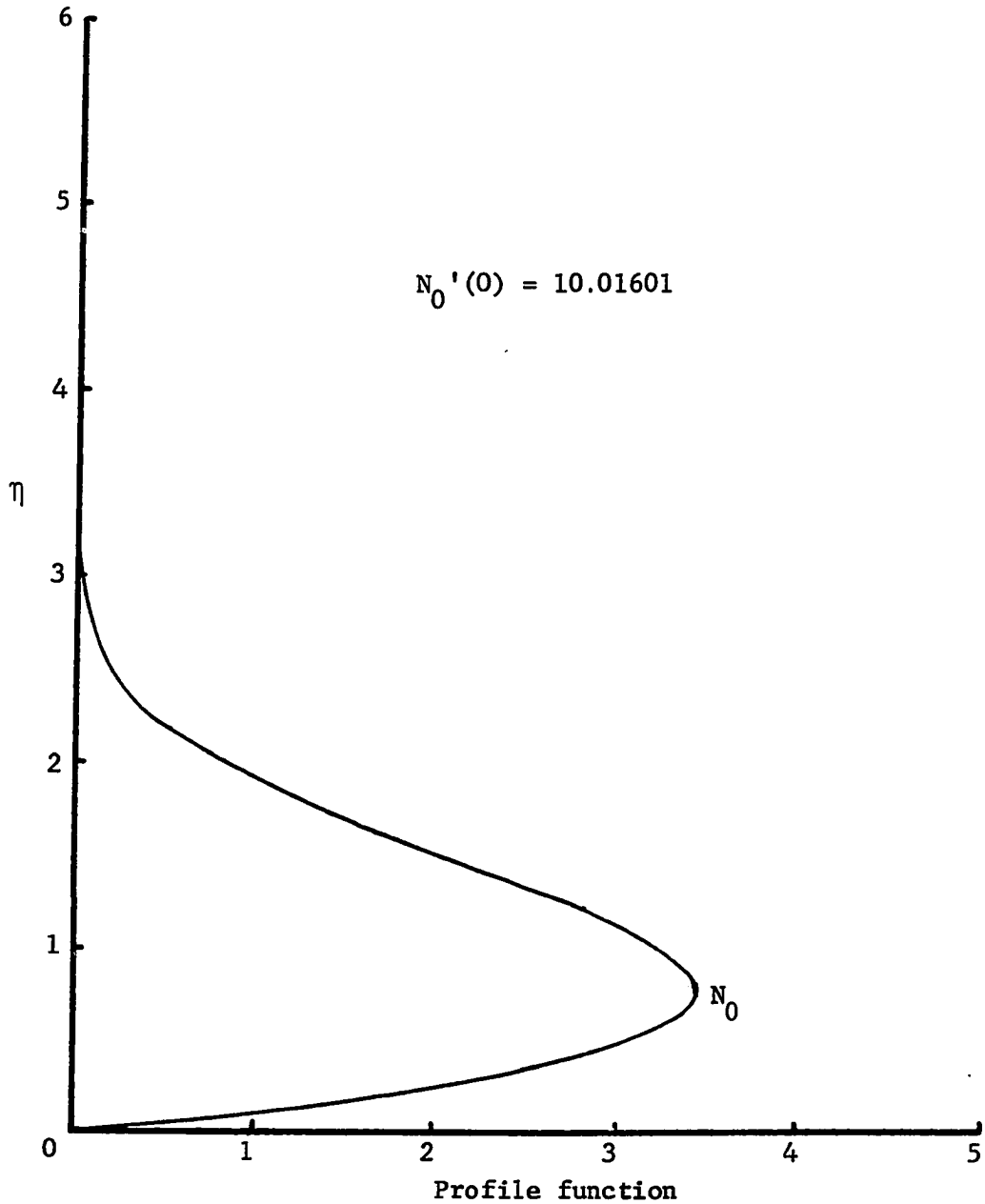

Figure 5. Profile function N_0 for a spinning cylinder

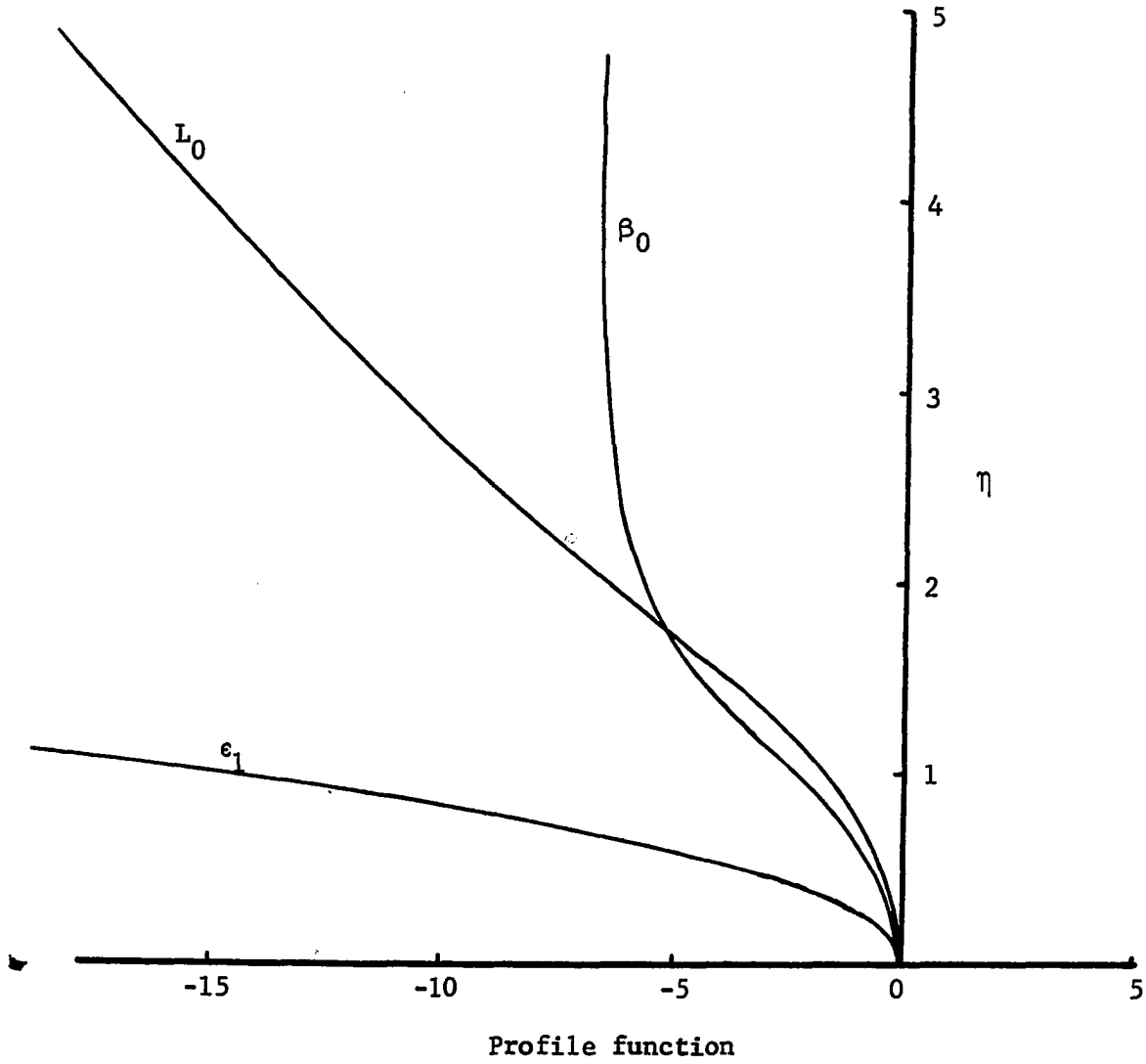

Figure 6. Velocity profile functions L_0, β_0 and ϵ_1 for a spinning cylinder

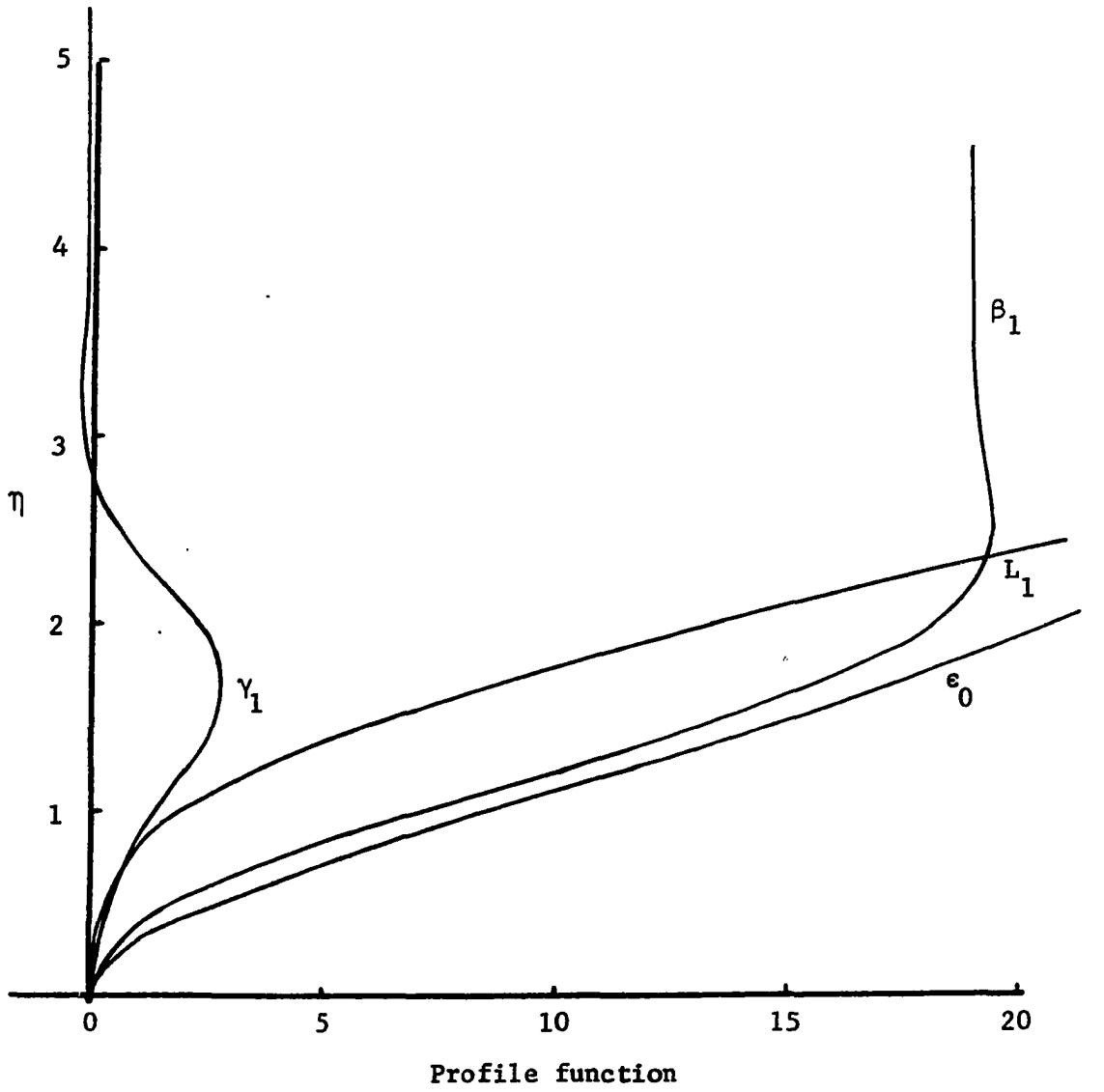

Figure 7. Velocity profile functions L_1, β_1, γ_1, and ϵ_0 for a spinning cylinder

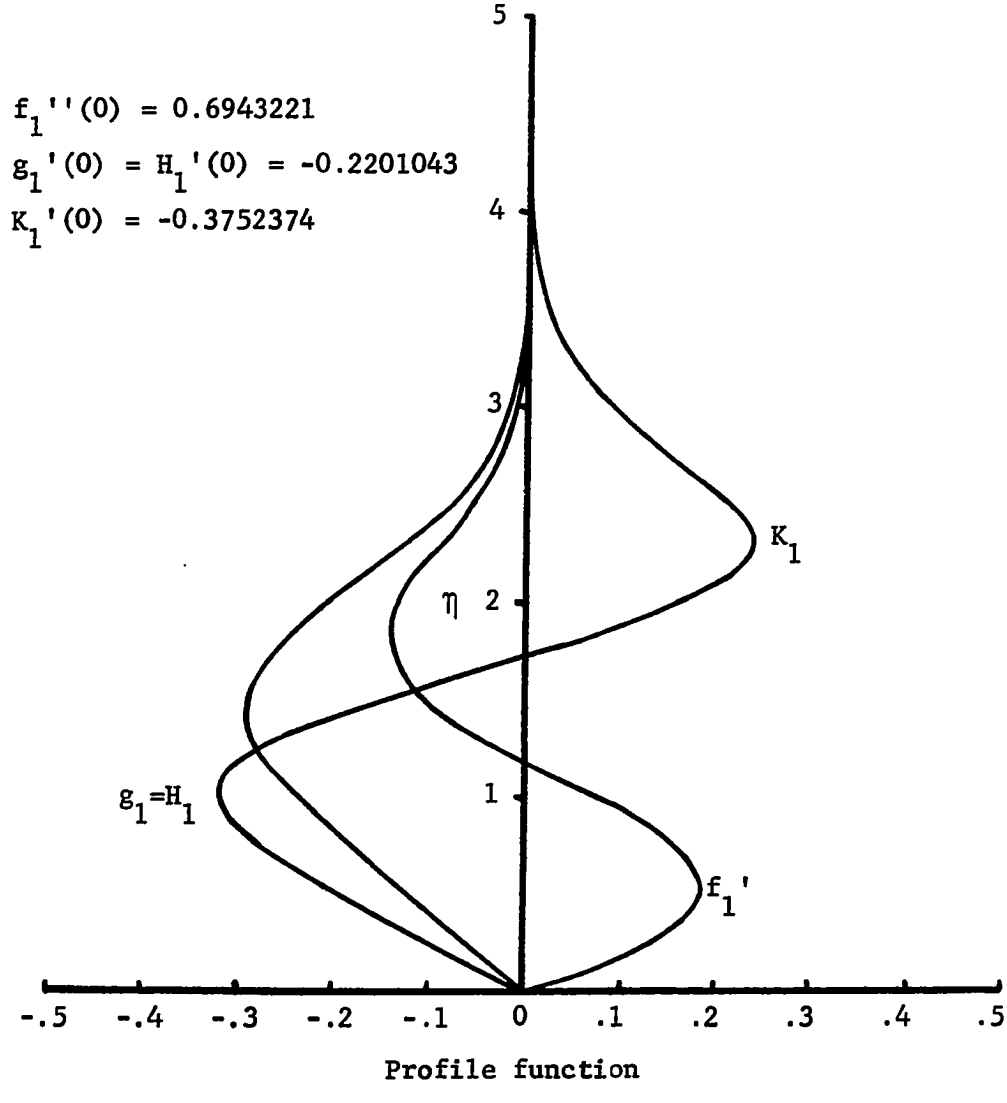

Figure 8. Velocity profile functions f_1', g_1, H_1 and K_1 for a spinning cylinder

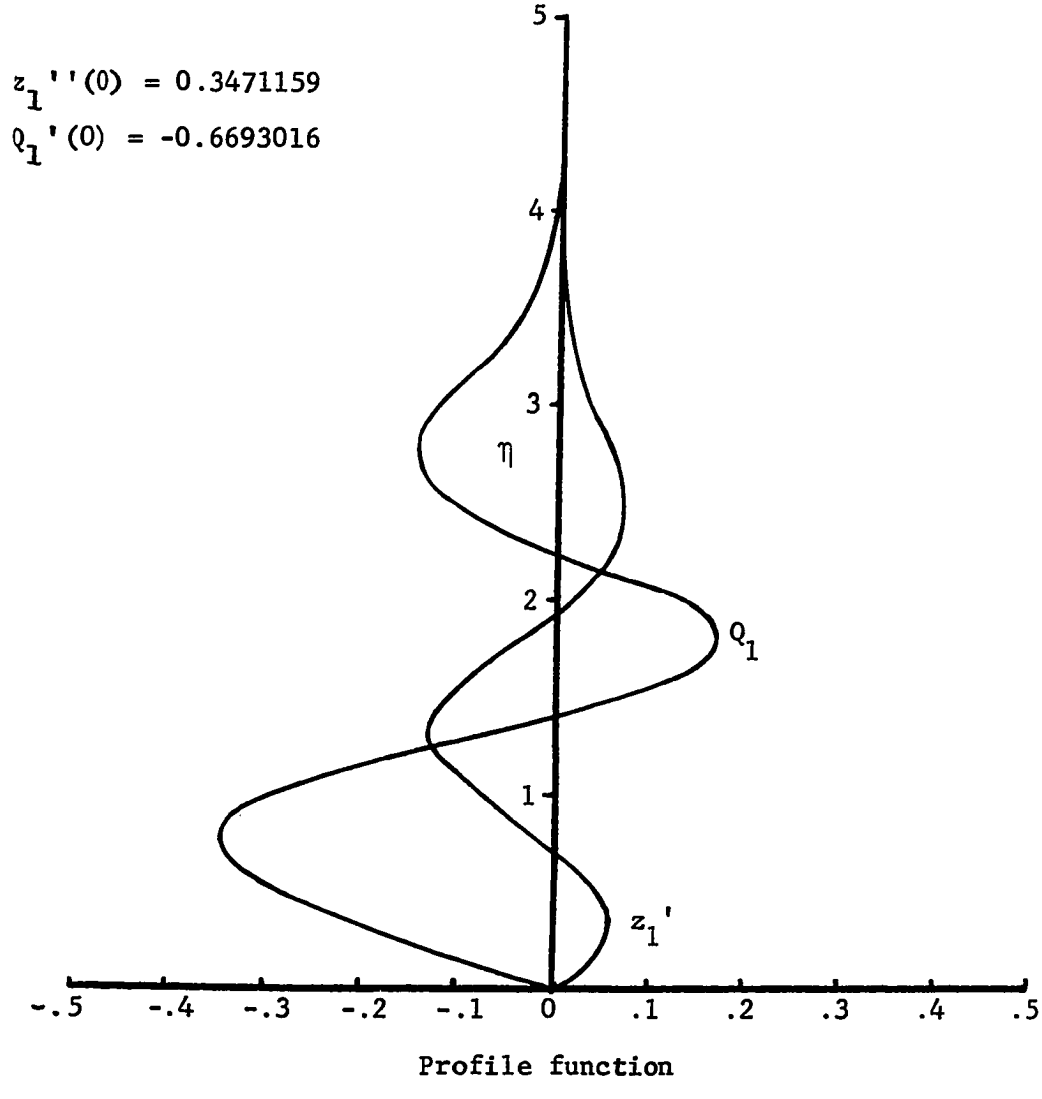

Figure 9. Velocity profile functions z_1' and Q_1 for a spinning cylinder

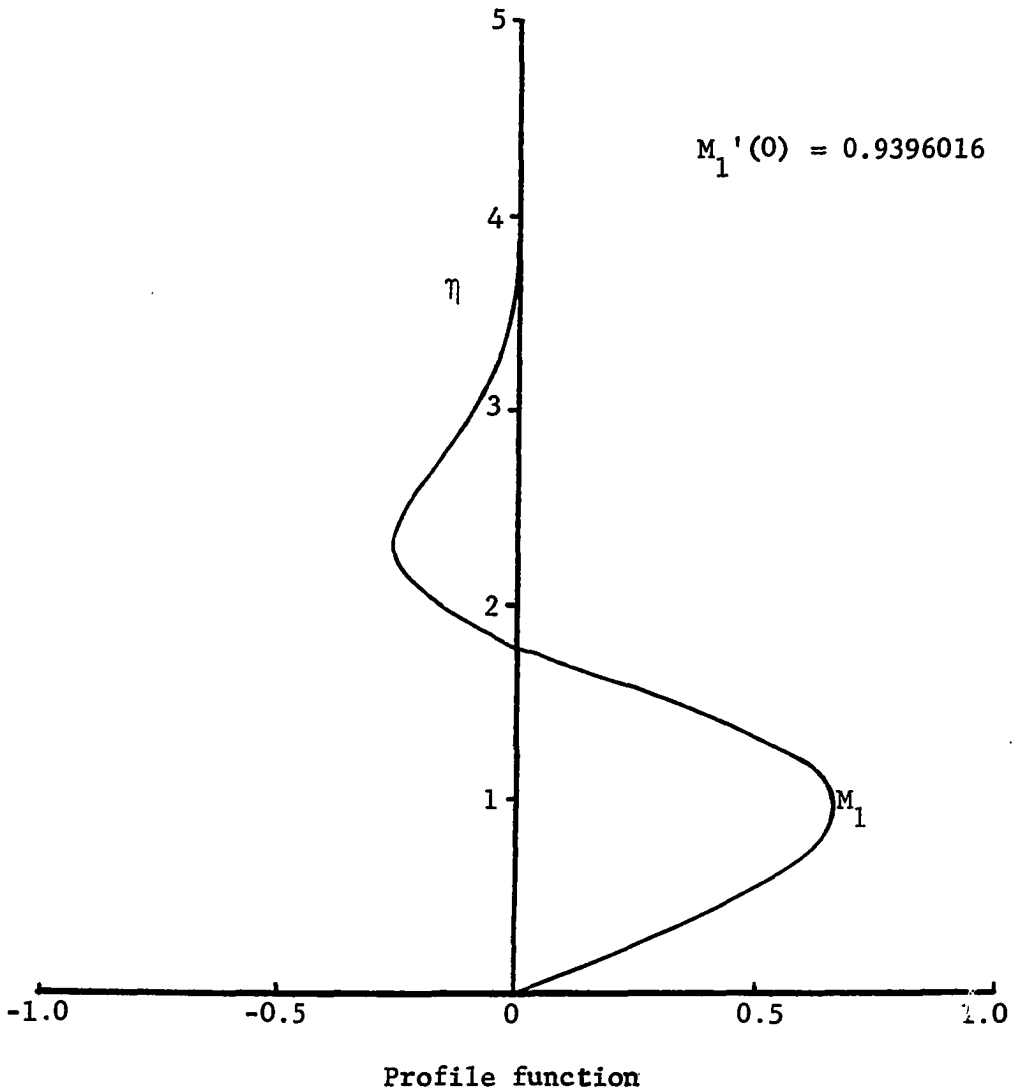

Figure 10. Velocity profile function M_1 for a spinning cylinder

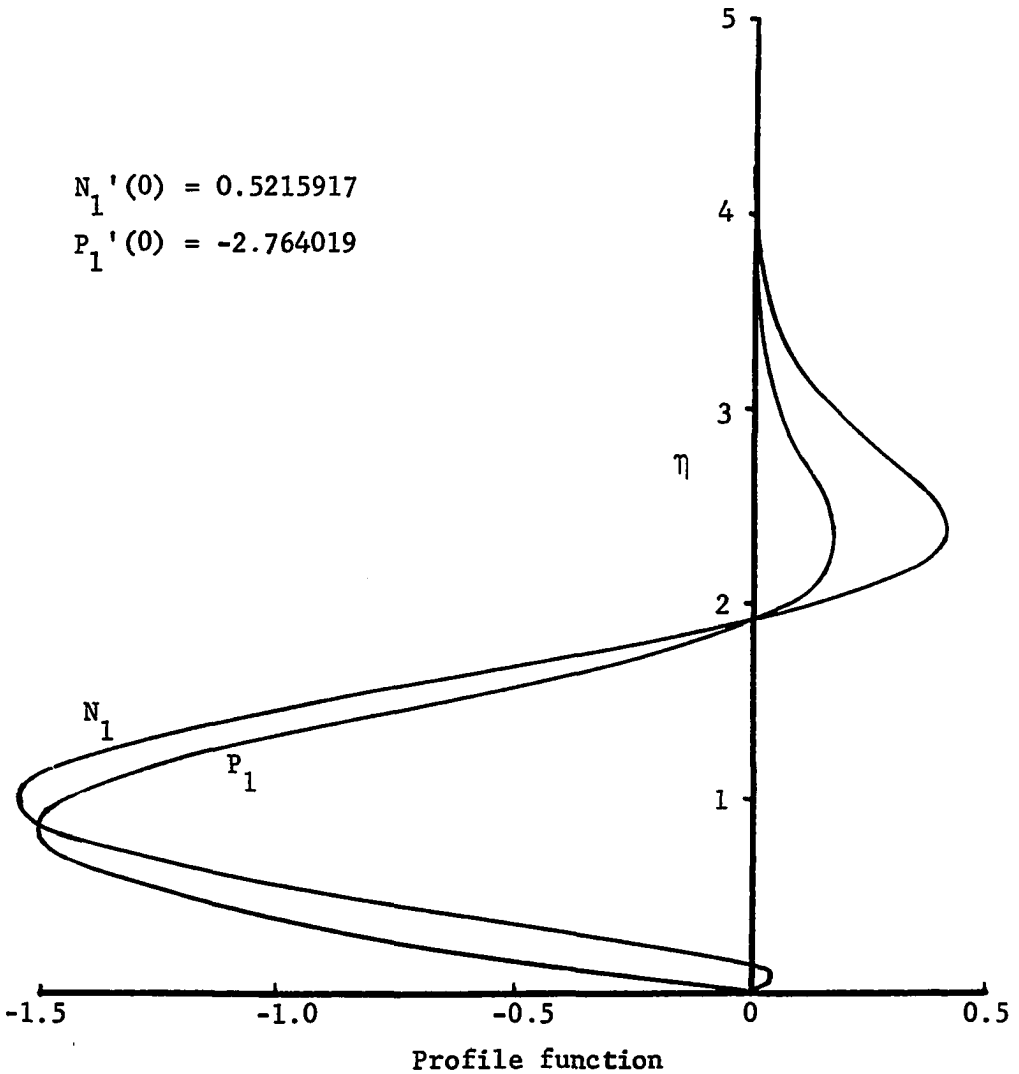

Figure 11. Velocity profile functions N_1 and P_1 for a spinning cylinder

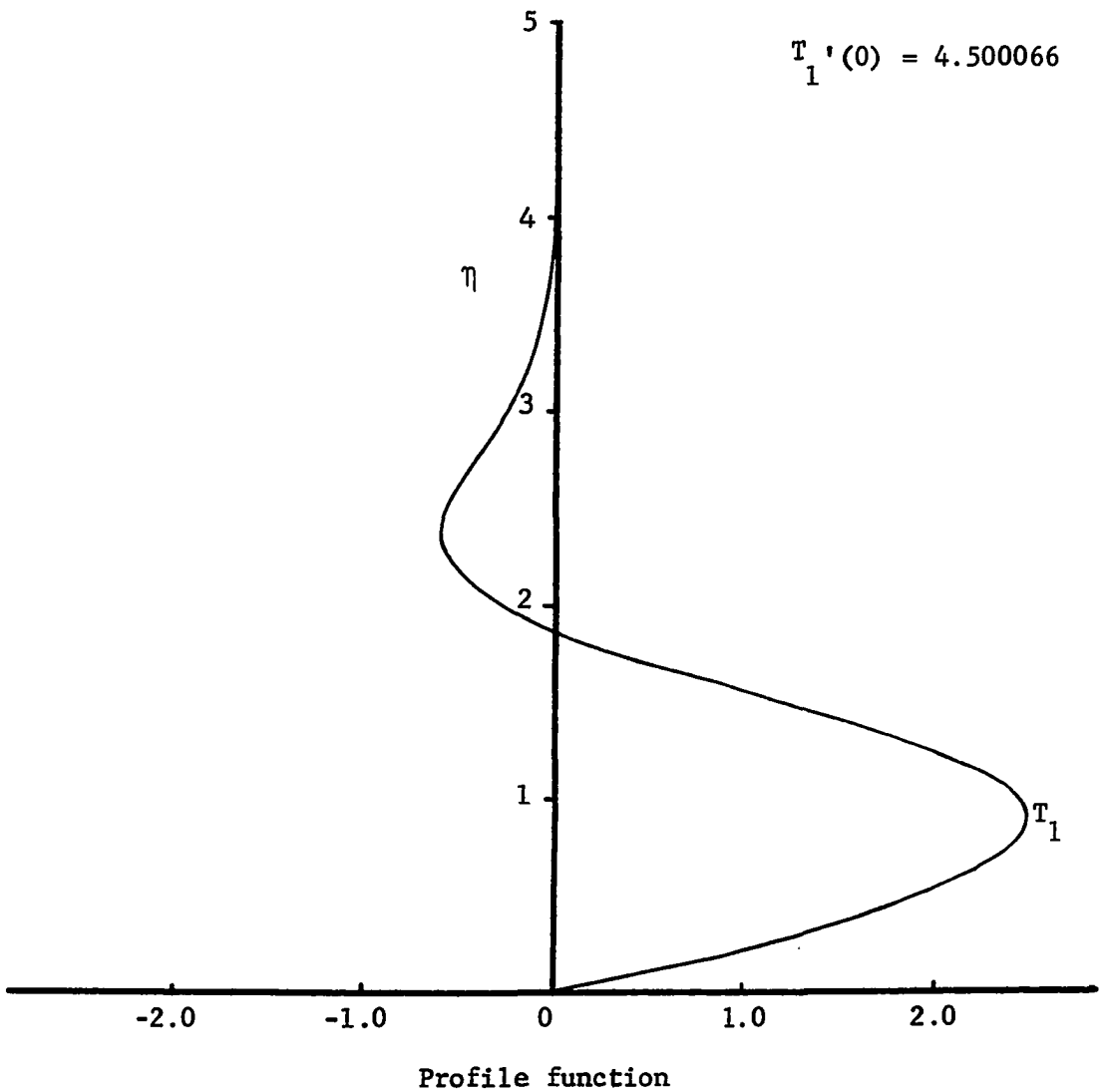

Figure 12. Velocity profile function T_1 for a spinning cylinder

The sideforce coefficient calculated to order ξ^2 is independent of the profile function of order ξ^2 except for the skin friction effect. The skin friction effect calculated to order ξ made only a small contribution to the total Magnus force. For this reason and since convergent solutions for some of the second order functions were not found, the second order term in the skin friction effect was neglected in the total Magnus force calculation.

Sideforce Calculations

The calculation of the Magnus force involves contributions due to the displacement thickness, the radial pressure gradient, skin friction, and the circulation distribution. The displacement thickness calculation involves an imaginary warped cylindrical body generated by adding the boundary layer displacement thickness to the cylinder. The solution for an inviscid flow about this new surface results in the appearance of a side force, the displacement thickness contribution to the total Magnus force. The displacement thickness effect is calculated assuming that the pressure throughout the boundary layer is constant in the radial direction. The radial pressure gradient contribution takes into account the pressure change from the outer edge of the boundary layer to the cylinder surface. The surface shearing stress is an asymmetric function of φ for the rotating cylinder. Integration of this shearing stress over the cylinder surface provides another contribution to the total Magnus force. The final contribution is that due to the axial circulation distribution caused by vorticity shed

into the crossflow wake. The local side force is related to the local circulation strength by Rayleigh's (18) theory for the lift on a rotating circular cylinder placed normal to the freestream. The total Magnus force, then, is obtained by integration of all local side force contributions over the length of the cylinder.

To calculate the displacement thickness of a three-dimensional boundary layer Moore's (15) definition in cylindrical coordinates is used

$$\left\{\int_{r_0}^{r_0+\Delta} u_1 r\,dr - \int_{r_0}^{r_0+\delta_1} (u_1-u)\,dr\right\}_x + \left\{\int_{r_0}^{r_0+\Delta} w_1\,dr - \int_{r_0}^{r_0+\delta_2} (w_1-w)\,dr\right\}_\varphi = 0 \tag{104}$$

where u_1 and w_1 are the inviscid flow velocities at the boundary layer edge

$$u_1 \cong U\left(1 - \frac{\alpha^2}{2}\right)$$
$$w_1 \cong U(2\alpha \sin\varphi - k\bar{p}) \tag{105}$$

δ_1 and δ_2 are the boundary layer thicknesses for the u and w profiles respectively. Δ is the desired displacement thickness. Transformation of Equation 104 to dimensionless coordinates yields

$$\left(1 - \frac{\alpha^2}{2}\right)\left\{\Delta + \frac{\Delta^2}{2r_0} - \frac{\xi r_0}{2}\int_0^\infty \left(1 - \frac{u}{U}\right) d\eta\right\}_x$$

$$+ \left\{(2\alpha \sin\varphi - k\bar{p})\left(\frac{\Delta}{r_0} - \frac{\eta_e}{2}\xi + \frac{\eta_e^2}{8}\xi^2\right)\right.$$

$$+ \frac{\xi}{2} \int_0^{\eta_e} \left(1 - \frac{\eta}{2} \xi\right) \frac{w}{U} \, d\eta \Bigg\}_{\varphi} = 0 \tag{106}$$

where η_e is the value of η at the boundary layer edge. Since δ is assumed to be much smaller than r_0, r is set equal to r_0 in Equations 101 and 103. This allows the determination of the velocities for substitution in Equation 106. To reduce Equation 106 to a set of ordinary differential equations it is assumed that Δ may be expanded in powers of α and $\bar{p}$ just as the velocity components were expanded previously.

$$\Delta = \zeta(x,\varphi) + \delta(x, \varphi, \alpha, \bar{p}) + \psi(x, \varphi, \alpha^2, \bar{p}^2, \alpha\bar{p}) \tag{107}$$

where

$$\begin{aligned} \zeta &= \zeta_0 + \xi\zeta_1 + \xi^2\zeta_2 \\ \delta &= \delta_0 + \xi\delta_1 + \xi^2\delta_2 \\ \psi &= \psi_0 + \xi\psi_1 + \xi^2\psi_2 \end{aligned} \tag{108}$$

For terms independent of α and $\bar{p}$ Equation 106 becomes

$$\left\{ \Delta + \frac{\Delta^2}{2r_0} - \frac{\xi r_0}{2} \int_0^{\infty} \left(1 - \frac{f_\eta}{2}\right) d\eta \right\}_x = 0 \tag{109}$$

Upon substitution of terms of Δ that are of zero order in α and $\bar{p}$ and expansion of the resulting equation in powers of ξ, Equation 109 may be directly integrated to yield

$$\zeta_0 = 0 \tag{110}$$

$$\zeta_1 = \frac{r_0 F_0}{2} \tag{111}$$

$$\zeta_2 = -\frac{r_0}{4}\left(\frac{F_0^2}{2} + F_1\right) \tag{112}$$

where

$$F_0 = \int_0^\infty \left(1 - \frac{f_0'}{2}\right) d\eta$$

$$F_1 = \int_0^\infty f_1' d\eta \tag{113}$$

The integrals F_0 and F_1 are readily calculated numerically from the known velocity profile functions and are constants.

For terms linear in α and $\bar{p}$ Equation 106 becomes

$$\left\{\Delta + \frac{\Delta^2}{2r_0} - \frac{\xi r_0}{2}\int_0^\infty \frac{x\alpha}{r_0}\cos\varphi\, K d\eta\right\}_x + \left\{(2\alpha\sin\varphi - k\bar{p})\left(\frac{\Delta}{r_0} - \frac{\eta}{2}\xi + \frac{\eta_e^2}{8}\xi^2\right)\right.$$

$$\left. + \frac{\xi}{2}\int_0^{\eta_e}\left(1 - \frac{\eta}{2}\xi\right)\left[\frac{\bar{p}}{2}(2-g) + \frac{\alpha}{2}[2+(.8604 - \eta)\xi]\sin\varphi H\right] d\eta\right\}_\varphi$$

$$= 0 \tag{114}$$

Direct integration of Equation 114 yields

$$\delta_0 = 0 \tag{115}$$

$$\delta_1 = -\frac{x\alpha}{2}\cos\varphi\, K_0 \tag{116}$$

$$\delta_2 = \frac{x\alpha}{2}\cos\varphi\left[\frac{F_0^2}{2} + F_1 - \bar{F}_0 - H_1 - .4302H_0 + \frac{\bar{H}_0}{2} + \frac{K_0F_0}{2} - K_1\right] \tag{117}$$

where

$$K_0 = \int_0^\infty K_0 d\eta$$

$$K_1 = \int_0^\infty K_1 d\eta$$

$$H_0 = \int_0^\infty H_0 d\eta \qquad (118)$$

$$H_1 = \int_0^\infty H_1 d\eta$$

$$\bar{F}_0 = \int_0^{\eta_e} \eta(1 - \frac{f_0'}{2})\, d\eta$$

$$\bar{H}_0 = \int_0^{\eta_e} \eta H_0 d\eta$$

The integrals are readily calculated from the known velocity profile functions and are constants.

For the second order terms $(\alpha^2, \alpha p, p^2)$ Equation 106 becomes

$$(1 - \frac{\alpha^2}{2}) \left\{ \Delta + \frac{\Delta^2}{2r_0} + \frac{\xi r_0}{2} \int_0^\infty \left[\frac{x^2\alpha^2}{r_0^2} (Q + \cos 2\varphi\Gamma) + \frac{x^2\alpha\bar{p}}{r_0^2} \sin\varphi P \right.\right.$$

$$\left.\left. - \frac{\alpha^2}{2} z_\eta \right] d\eta + \frac{\xi r_0}{2} \int_0^\infty (1 - \frac{f_\eta}{2})\, d\eta \right\}_x$$

$$+ \left\{ (2\alpha \sin\varphi - k\bar{p}) (\frac{\Delta}{r_0} - \frac{\eta_e}{2}\xi + \frac{\eta_e^2}{8}\xi^2) \right.$$

$$+ \frac{\xi}{2} \int_0^0 (1 - \frac{\eta}{2}\xi) \left[\frac{x\alpha\bar{p}}{r_0} \cos \varphi M + \frac{x\alpha^2}{2r_0} \sin 2\varphi N \right] d\eta \Bigg\}_{\varphi} = 0 \quad (119)$$

Then the solution of Equation 119 may be written:

$$\psi_0 = 0 \quad (120)$$

$$\psi_1 = - \frac{x^2\alpha^2}{2r_0} Q_0 + \frac{r_0\alpha^2}{4} Z_0 + x\alpha \cos\varphi \eta_e + \frac{x^2\alpha\bar{p}}{4r_0} \sin\varphi(M_0 - 2P_0)$$

$$- \frac{x^2\alpha^2}{4r_0} \cos 2\varphi \, (2T_0 - 2K_0 + N_0) \quad (121)$$

$$\psi_2 = \frac{x^2\alpha^2}{4r_0} (F_0 Q_0 - 2Q_1) - \frac{r_0\alpha^2}{8} (F_0 Z_0 + 2Z_1) - \frac{x\alpha}{2} \cos\varphi \, \eta_e (F_0 + \frac{\eta_e}{2})$$

$$- \frac{x^2\alpha\bar{p}}{8r_0} \sin\varphi \left[F_0(M_0 - 2P_0) + 4P_1 - 2M_1 - \bar{M}_0 \right]$$

$$+ \frac{x^2\alpha^2}{8r_0} \cos 2\varphi \left[F_0(T_0 - 2K_0 + N_0) - 4T_1 + 4N_1 - \bar{N}_0 \right] \quad (122)$$

---

where

$$M_0 = \int_0^\infty M_0 d\eta$$

$$N_0 = \int_0^\infty N_0 d\eta$$

$$P_0 = \int_0^\infty P_0 d\eta$$

$$Q_0 = \int_0^\infty Q_0 d\eta$$

$$T_0 = \int_0^\infty T_0 d\eta$$

$$Z_0 = \int_0^\infty Z_0 d\eta$$

$$\bar{M}_0 = \int_0^\infty M_0 d\eta$$

$$\bar{N}_0 = \int_0^\infty N_0 d\eta \qquad (123)$$

$$M_1 = \int_0^\infty M_1 d\eta$$

$$N_1 = \int_0^\infty N_1 d\eta$$

$$P_1 = \int_0^\infty P_1 d\eta$$

$$Q_1 = \int_0^\infty Q_1 d\eta$$

$$T_1 = \int_0^\infty T_1 d\eta$$

$$Z_1 = \int_0^\infty Z_1 d\eta$$

These integrals may be calculated from the known velocity profile functions and are also constants.

Only terms containing $\sin \varphi$ contribute to the asymmetry of the displace-

ment thickness with respect to the vertical plane. For this reason the Magnus force is dependent on these terms only. The Magnus displacement thickness is, then

$$\Delta_M = \alpha\bar{p}\,\left(\frac{x}{r_0}\right)^2\sqrt{\frac{\nu x}{U}}\,\sin\varphi\left\{(M_0 - 2P_0) - \frac{2}{r_0}\sqrt{\frac{\nu x}{U}}\left[4P_1 - 2M_1 + M_0(1 + F_0) - 2P_0F_0\right]\right\} \tag{124}$$

Upon application of the Munk-Jones (20) theory to the case of flow over slender bodies of revolution at incidence, the generated displacement thickness distorts the velocity potential by an amount

$$\varphi = -U\,\frac{\partial\Delta_M}{\partial x}\,\frac{R_0^2}{r} \tag{125}$$

where R_0 is the radius of the new surface. The surface pressure coefficient is then

$$C_{P_0} = -\frac{2\varphi_x}{U} = \frac{\alpha\bar{p}}{r_0}\sqrt{\frac{\nu x}{U}}\,\sin\varphi\left\{\frac{15}{2}(M_0 - 2P_0) - \frac{8}{r_0}\sqrt{\frac{\nu x}{U}}\,(12P_1 - 6M_1 + 3M_0 - 2F_0M_0 - 4F_0P_0)\right\} \tag{126}$$

and, thus, the force per unit length

$$y = -q\int_0^{2\pi} C_{P_0}\,r_0\,\sin\varphi\,d\varphi \tag{127}$$

may be integrated along the body to calculate the Magnus side force contribution Y_1 due to the displacement thickness

$$Y_1 = \int_0^L y\,dx \tag{128}$$

The side force coefficient based on the cross sectional area is, then

$$C_{Y_1} = \frac{8\alpha\bar{p}}{R_L^{\frac{1}{2}}}\left(\frac{L}{d}\right)^2\left\{-\frac{15}{6}(M_0 - 2P_0) + \frac{4}{R_L^{\frac{1}{2}}}\left(\frac{L}{d}\right)(12P_1 - 6M_1 - 3\bar{M}_0 - 2F_0M_0 + 4F_0P_0)\right\} \tag{129}$$

The radial pressure gradient contribution to the Magnus force is calculated using the r component of the momentum equation correct to order (δ/L).

$$\frac{w^2}{r} = -\frac{P_r}{\rho} \tag{130}$$

The velocity profile Equation 103 can then be substituted into Equation 130. The resulting equation for the radial pressure gradient is transformed to dimensionless coordinates. Since only pressure gradient terms with sin φ asymmetry will contribute to the Magnus force, the Magnus pressure gradient is

$$P_\eta = \rho U^2\sqrt{\frac{\nu x}{U}}\frac{\alpha\bar{p}\sin\varphi}{r_0}\left\{(2 - f_0')f_0'\left[1 + .8604(\xi - \xi^2)\right] - \left(\frac{k}{\xi^2}\right)f_0'\xi^2\right\} \tag{131}$$

The radial pressure gradient contribution to the side force per unit length is calculated by

$$y_2 = \int_0^{2\pi} r_0 \sin\varphi \int_1^\infty P_\eta d\eta\, d\varphi \tag{132}$$

Defining

$$F_3 = \int_0^{\infty} (2 - f_0')f_0' \, d\eta$$

$$F_4 = \int_0^{\eta_e} f_0' \, d\eta \tag{133}$$

and calculating the side force using

$$Y_2 = \int_0^{L} y_2 dx \tag{134}$$

results in the radial pressure gradient contribution to the Magnus side-force coefficient based on the cross sectional area

$$C_{Y_2} = \frac{8}{R_L^{\frac{1}{2}}} \left(\frac{L}{d}\right)^2 \alpha p \left\{ F_3 \left[\frac{2}{3} + \frac{3.4428}{R_L^{\frac{1}{2}}} \left(\frac{L}{d}\right) - \frac{22.0339}{R_L} \left(\frac{L}{d}\right)^2 \right] - \frac{64}{R_L} \left(\frac{L}{d}\right)^2 F_4 C_1 R_C^{3/4} \right\} \tag{135}$$

The integrals F_3 and F_4 are readily calculated numerically from the known velocity profile functions and are constants.

The skin friction contribution to the Magnus force per unit length is calculated by

$$y_3 = \int_0^{2\pi} r_0 \, \tau \cos \varphi \, d\varphi \tag{136}$$

where τ is the surface shearing stress

$$\tau = \mu w_r / r=r_0 \tag{137}$$

Equation 103 is substituted into Equation 137. Note that only the terms involving cos φ will be nonzero after integration so the shearing stress

that contributes to the Magnus force is

$$\tau_M = \frac{\mu U x}{2 r_0}\sqrt{\frac{U}{\nu x}}\,\bar{\alpha p}\cos\varphi\left(M_0' + \frac{4}{r_0}\sqrt{\frac{\nu x}{U}}\,M_1' + \frac{16}{r_0^2}\,\frac{\nu x}{U}\,M_2'\right)\Bigg|_{\eta=0} \qquad (138)$$

Substituting this result into Equation 136 and integrating, the Magnus force per unit length y_3 is found. The total force is

$$Y_3 = \int_0^L y_3\,dx$$

from which the skin friction contribution to the side force coefficient is calculated to be

$$C_{Y_3} = \frac{8}{3}\left(\frac{L}{d}\right)^2 \frac{1}{R_L^{1/2}}\,\bar{\alpha p}\left\{M_0' - \frac{4}{R_L^{1/2}}\left(\frac{L}{d}\right)M_1' + 25.6\left(\frac{L}{d}\right)^2\frac{1}{R_L}\,M_2'\right\} \qquad (139)$$

The derivatives of the profile function M are known from the velocity profile solutions and are constant.

The contribution to the Magnus side force due to the circulation distribution is calculated by

$$Y_4 = \int_0^L \rho U\,\alpha\,k(x)\,\Gamma_0\,dx \qquad (140)$$

Since the circulation distribution has the form

$$k(x) = C_1 R_C^{3/4}\,\xi^2 \qquad (141)$$

the Magnus side force coefficient due to the circulation distribution is

$$C_{Y_4} = 256\,C_1\,\frac{R_C^{3/4}}{R_L}\left(\frac{L}{d}\right)^3\bar{\alpha p} \qquad (142)$$

RESULTS AND DISCUSSION

The contribution to the Magnus force coefficient due to the displacement thickness is

$$C_{Y_1} = \frac{8\alpha\bar{p}}{R_L^{\frac{1}{2}}} \left(\frac{L}{d}\right)^2 \left\{ -\frac{15}{6} (\mathcal{M}_0 - 2\mathcal{P}_0) + \frac{4}{R_L^{\frac{1}{2}}} \left(\frac{L}{d}\right) (12\mathcal{P}_1 - 6\mathcal{M}_1 - 3\bar{\mathcal{M}}_0 - 2F_0\mathcal{M}_0 + 4F_0\mathcal{P}_0) \right\} \tag{127}$$

where the numerical values for the integrals of the velocity profile functions have the values

$$\begin{aligned} F_0 &= 0.8604 \\ \mathcal{M}_0 &= -1.3800 \\ \bar{\mathcal{M}}_0 &= -1.6094 \\ \mathcal{P}_0 &= 0.7630 \\ \mathcal{M}_1 &= 0.4826 \\ \mathcal{P}_1 &= -1.5910 \end{aligned} \tag{143}$$

Substitution of these values into Equation 127 yields

$$C_{Y_1} = \frac{\alpha\bar{p}}{R_L^{\frac{1}{2}}} \left(\frac{L}{d}\right)^2 \left\{ 58.1200 - \frac{389.0816}{R_L^{\frac{1}{2}}} \left(\frac{L}{d}\right) \right\} \tag{144}$$

The contribution to the Magnus force coefficient due to the radial pressure gradient is

$$C_{Y_2} = \frac{8\alpha\bar{p}}{R_L^{\frac{1}{2}}} F_3 \left(\frac{L}{d}\right)^2 \left\{ \frac{2}{3} + \frac{3.4428}{R_L^{\frac{1}{2}}} \left(\frac{L}{d}\right) - \frac{22.0339}{R_L} \left(\frac{L}{d}\right)^2 \right\} \tag{133}$$

The numerical value of F_3 is

$$F_3 = 1.2883 \tag{145}$$

Substitution of this value into Equation 133 yields

$$C_{Y_2} = \frac{\alpha\bar{p}}{R_L^{\frac{1}{2}}} \left(\frac{L}{d}\right)^2 \left\{ 6.8709 + \frac{35.4705}{R_L^{\frac{1}{2}}} \left(\frac{L}{d}\right) - \frac{227.0112}{R_L} \left(\frac{L}{d}\right)^2 \right\} \tag{146}$$

The contribution to the Magnus force coefficient due to the skin friction is

$$C_{Y_3} = \frac{8}{3} \frac{\alpha\bar{p}}{R_L^{\frac{1}{2}}} \left(\frac{L}{d}\right)^2 \left\{ M_0' - \frac{4}{R_L^{\frac{1}{2}}} \left(\frac{L}{d}\right) M_1' \right\} \tag{137}$$

The derivatives of the velocity profile function M have the values

$$\begin{aligned} M_0' &= -1.5057 \\ M_1' &= 0.9396 \end{aligned} \tag{147}$$

Substitution of these values into Equation 137 yields

$$C_{Y_3} = \frac{\alpha\bar{p}}{R_L^{\frac{1}{2}}} \left(\frac{L}{d}\right)^2 \left\{ -4.0152 - \frac{3.7584}{R_L^{\frac{1}{2}}} \left(\frac{L}{d}\right) \right\} \tag{148}$$

The contribution to the Magnus force coefficient due to the circulation distribution is

$$C_{Y_4} = \frac{256\, C_1 R_C^{3/4}}{R_L} \left(\frac{L}{d}\right)^3 \alpha\bar{p} \tag{140}$$

where

$$C_l = .0328 \qquad \left(\frac{\bar{p}}{\sin\alpha} \leqq 0.25\right)$$

$$= .0015 + .0394\,\frac{\alpha}{p} \qquad \left(\frac{\bar{p}}{\sin\alpha} \geqq 7.0\right) \tag{149}$$

Substitution of these results into Equation 140 yields

$$C_{Y_4} = 8.3968\, R_C^{3/4}\, \frac{\alpha\bar{p}}{R_L} \left(\frac{L}{d}\right)^3 \qquad \left(\frac{p}{\sin\alpha} \leqq 0.25\right)$$

$$= \left(.3840 + 10.0864\,\frac{\alpha}{p}\right) R_C^{3/4}\, \frac{\alpha\bar{p}}{R_L} \left(\frac{L}{d}\right)^3 \qquad \left(\frac{\bar{p}}{\sin\alpha} \geqq 7.0\right) \tag{150}$$

The total Magnus force coefficient is thus

$$C_{Y_I} = \frac{\alpha\bar{p}}{R_L^{1/2}} \left(\frac{L}{d}\right)^2 \left\{60.9757 + \frac{1}{R_L^{1/2}} \left(\frac{L}{d}\right)\left[-357.3695 + 8.3968\, R_C^{3/4}\right] - \frac{227.0112}{R_L} \left(\frac{L}{d}\right)^2\right\} \qquad \left(\frac{\bar{p}}{\sin\alpha} \leqq 0.25\right) \tag{151}$$

or

$$C_{Y_{II}} = \frac{\alpha\bar{p}}{R_L^{1/2}} \left(\frac{L}{d}\right)^2 \left\{60.9757 + \frac{1}{R_L^{1/2}} \left(\frac{L}{d}\right)\left[-357.3695 + \left(.3840 + 10.0864\,\frac{\alpha}{p}\right) R_C^{3/4}\right] - \frac{227.0112}{R_L} \left(\frac{L}{d}\right)^2\right\}$$

$$\left(\frac{p}{\sin\alpha} \geqq 7.0\right) \tag{152}$$

For subsonic incompressible flow with α and $\bar{p}$ small Equation 152 would be expected to be the most useful equation for determining the Magnus force.

Figures 13 and 14 show a comparison of the present result, Kelly and Hauer's (12) wind tunnel data and Kelly's (10) result for the Magnus

force developed by a cylinder for various $\bar{p}$ and L/d values. Kelly's result predicts a linear variation of the sideforce coefficient with α for a given $\bar{p}$. The data indicates that this is only valid for very small α. The addition of the circulation distribution to the theory greatly improves Kelly's result for larger α's. The present result is much better in predicting wind tunnel sideforce values than Kelly's theory at all angles of attack. The present result does not always compare favorably with experimental data but since the sideforce magnitude is much smaller than the other forces acting on the cylinder, accurate wind tunnel data are very difficult to obtain. Often quite different results for experimental Magnus force coefficients are obtained between tests run at positive and negative spin rates. Varying the nose shape or testing in a different wind tunnel can also have large effects on the experimental results. Equation 152 predicts the shape of the sideforce coefficient, however, very well even beyond the expected small angle region of application. No other theoretical application to date has predicted other than a linear variation of Magnus force coefficient C_Y with angle of attack at a constant $\bar{p}$.

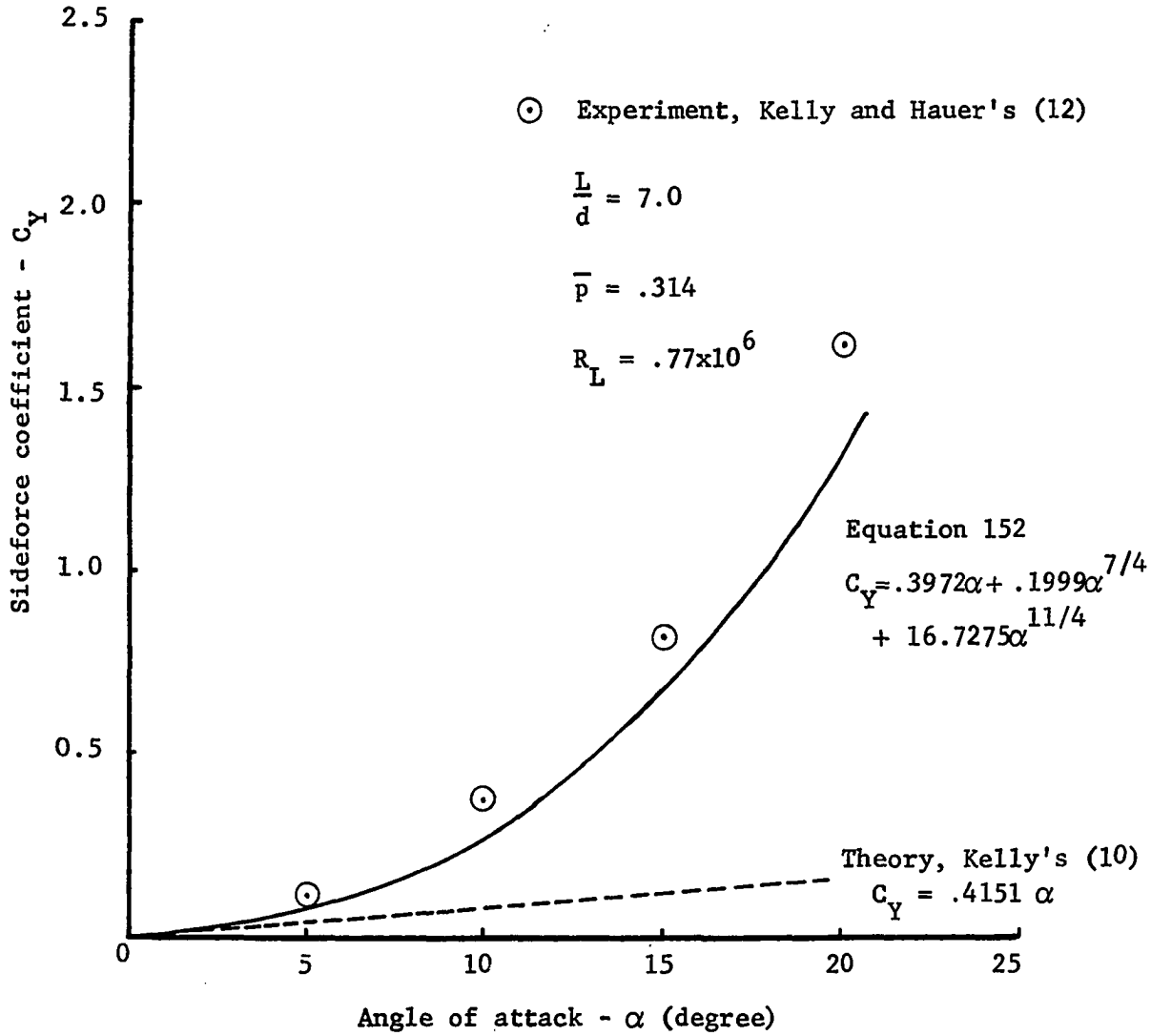

Figure 13. Sideforce coefficient comparison

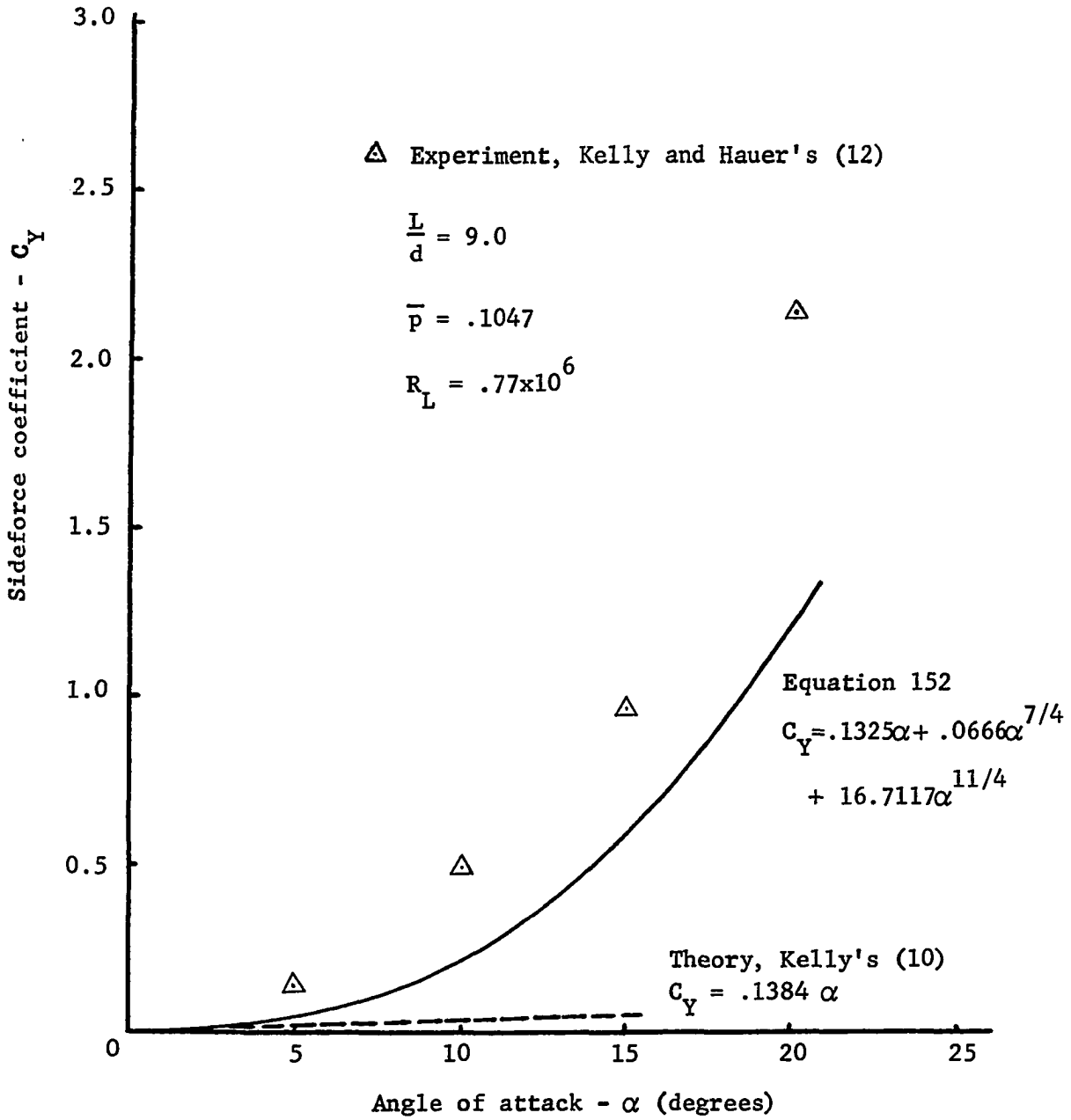

Figure 14. Sideforce coefficient comparison

CONCLUSIONS AND RECOMMENDATIONS

This study of Magnus force production of spinning cylinders at small angles of attack has lead to the following conclusions:

1. A circulation is developed in the inviscid outer flow by shed vorticity in the wake of a spinning rotating cylinder.

2. The boundary layer displacement thickness is affected little by a superimposed circulation distribution.

3. The use of a crossflow similar to the flow over an impulsively rotated cylinder placed normal to the freestream yields reasonable results for the prediction of the sideforce coefficient.

4. Effects due to terms of first order in ξ yield important contributions to the sideforce coefficient and should not be neglected.

5. For large angles of attack the sideforce is produced mainly by the circulation induced in the inviscid flow by the shed vorticity.

6. Equation 152 predicts the nonlinear behavior of the sideforce coefficient that previous theories have not.

7. Equation 152 may even be useful in the estimation of the sideforce coefficient above the assumed "small" angle of attack region.

8. Although there are wind tunnel tests that have been made on finless rotating bodies of revolution in addition to those referenced here, many more experimental results are needed to confirm the results contained herein. Wide ranges of $\bar{p}$, α, L/d, Reynolds number and Mach

number should be covered by these experiments to fill in gaps in existing data.

9. Flow field surveys with a hot wire should be made to validate the assumed circulation values and to better understand the flow characteristics, particularly in the wake region where vorticity is shed from the boundary layer.

10. When reliable wind tunnel data are available an extensive comparison of the theory and experiment should be made to determine the validity of the theory.

REFERENCES CITED

1. Buford, W. E. Magnus Effect in the Case of Rotating Cylinders and Shell. U.S. AEC Report MR 821 (Ballistic Research Laboratories, Aberdeen Proving Ground, Md.) July, 1954.

2. Crane, R. L. Stability and Local Accuracy of Numerical Methods for Ordinary Differential Equations. Ph.D. thesis. Ames, Iowa, Library, Iowa State University of Science and Technology.

3. Dunn, E. L. A Low-Speed Experimental Study of Yaw Forces on Bodies of Revolution at Large Angles of Pitch and Zero Angle of Sideslip. U.S. AEC Report TM-1588 (U.S. Naval Ordnance Test Station, China Lake, California). March, 1954.

4. Glauert, M. B. The Flow Past a Rapidly Rotating Circular Cylinder. Royal Society of London Proceedings, Series A, 242:108-115. November, 1957.

5. Gowen, F. E. and Perkins, E. W. Flow Over Inclined Bodies. U.S. AEC Report NACA RM A51J25 (Ames Aeronautical Laboratory, Moffet Field, California) November, 1951.

6. Howarth, L. Note on the Boundary Layer on a Rotating Sphere. Philosophical Magazine 42, 7th Series:1308-1315. November, 1951.

7. Illingworth, C. R. Boundary Layer Growth on a Spinning Body. Philosophical Magazine 45:1-8. October, 1953.

8. Iversen, J. D. Private Communication. 1971.

9. Kelly, H. R. The Estimation of Normal-Force, Drag, and Pitching Moment Coefficients for Blunt-Based Bodies of Revolution at Large Angles of Attack. Journal of the Aeronautical Sciences 21:549. August, 1954.

10. Kelly, H. R. An Analytical Method for Predicting the Magnus Forces and Moments on Spinning Projectiles. U.S. AEC Report TM-1634. (U.S. Naval Ordnance Test Station, China Lake, California) 1954.

11. Kelly, H. R. and Thacker, G. R. The Effect of High Spin on the Magnus Force on a Cylinder at Small Angles of Attack. U.S. AEC Report NOTS 1381, NAVORD Report 5036 (U.S. Naval Ordnance Test Station, China Lake, California) 1956.

12. Kelly, H. R. and Hauer, H. J. The Subsonic Aerodynamic Characteristics of Spinning Cone-Cylinders and Ogive-Cylinders at Large Angles of Attack. U.S. AEC Report NOTS 1166 (U.S. Naval Ordnance Test Station, China Lake, California) 1955.

13. Magnus, G. Uber die Aberwucheing der Geschosie. Abhandle d. Klg. Akad d. Wiss zer Berlin, Poggendorffs Annelen der Physiks 88, I. 1853.

14. Martin, J. C. On Magnus Effects Caused by the Boundary Layer Displacement Thickness of Bodies of Revolution at Small Angles of Attack. U.S. AEC Report BRL R870 (Ballistic Research Laboratories, Aberdeen Proving Ground, Md.) September, 1956.

15. Moore, F. K. Displacement Effect of a Three-Dimensional Boundary Layer. U.S. AEC Report NACA TN 2722 (Lewis Flight Propulsion Laboratory, Cleveland, Ohio) June, 1952.

16. Platou, A. S. Magnus Characteristics of Finned and Nonfinned Projectiles. AIAA Journal 3, No. 1:83-90. January, 1965.

17. Prandtl, L. Application of the Magnus Effect to the Wind Propulsion of Ships (Translation). AEC Report NACA TM 367 (National Aeronautics and Space Administration, Washington, D.C.) 1924.

18. Lord Rayleigh. On the Irregular Flight of a Tennis Ball. Messenger of Mathematics 7:14. 1877.

19. Robins, B. New Principles of Gunnery. London. 1842.

20. Sears, W. R. Small Perturbation Theory. Princeton University Press, Princeton, N.J. 1960.

21. Sieron, T. R. On the Magnus Effects of an Inclined Spinning Shell at Subsonic and Transonic Speeds. U.S. AEC Report WAAD TR 60-212 (Aeronautical Systems Division, Wright-Patterson Air Force Base, Ohio) April, 1961.

22. Thoman, D. C. and Szewczyk, A. A. Numerical Solutions of Time Dependent Two-Dimensional Flow of a Viscous, Incompressible Fluid Over Stationery and Rotating Cylinders. Report TR66-14. Department of Mechanical Engineering, University of Notre Dame (Notre Dame, Indiana) July, 1966.

23. Wood, W. W. Boundary Layers Whose Streamlines are Closed. Aeronautical Research Laboratories, Fishermans Bend, Melbourne, Australia. September, 1956.

ACKNOWLEDGMENTS

The author wishes to express his sincere gratitude to Professor J. D. Iversen for his guidance and assistance in the preparation of this dissertation.

Acknowledgment is also given to Dr. E. W. Anderson for his help in preparing the draft of this dissertation and to my wife, Beverly, for the typing of the manuscript.